



Cite this: *J. Mater. Chem. A*, 2025, **13**, 39586

## Removal of radioactive elements from nuclear wastewater using metal–organic frameworks: a comprehensive analysis using DFT and meta-analysis

Q.-L. Huang,<sup>a</sup> X.-M. Chen,<sup>a</sup> Q.-R. Zhang,<sup>ID \*a</sup> J.-Y. Lim,<sup>b</sup> S.-W. Zhao,<sup>a</sup> H.-X. Guan,<sup>c</sup> S. Wang<sup>d</sup> and J.-Q. Liu<sup>ID \*c</sup>

Metal–organic frameworks (MOFs) have great potential in nuclear wastewater treatment. In this study, based on research data from 2016 to 2025, the structural properties of various types of MOFs and their complexes were systematically evaluated, highlighting performance differences under different experimental conditions, with special emphasis on the central role of structural stability. The mechanism by which solvation in aqueous media influences the stability of MOFs was revealed by combining density-functional theory (DFT) calculations with experimental data validation. Through a comparative parametric analysis of 25 key studies, it was found that the adsorption efficiency of MOFs for radioactive elements is closely related to their synthesis method and environmental conditions. It is further suggested that the stability, reproducibility, and adsorption capacity of the materials can be significantly enhanced by modification, while reducing environmental risks. This study also evaluates the commercialization prospects and eco-friendliness of MOF materials and provides a theoretical basis for the secondary utilization of radioactive metal cations, aiming to provide scientific references for the design of MOF materials targeting the removal of radioactive ions and their application in the remediation of complex natural water bodies.

Received 28th May 2025

Accepted 26th August 2025

DOI: 10.1039/d5ta04304b

rsc.li/materials-a

## 1. Introduction

As global warming and fossil fuel depletion become increasingly serious issues, nuclear energy becomes an appealing alternative energy source since it is low-cost, sustainable, and efficient.<sup>1</sup> The economic and ecological viability of nuclear power remains unknown, with one key environmental issue linked to the nuclear fuel cycle being the development of radioactive byproducts, which poses chemical and radiological risks to humankind. They represent a long-term hazard to surface and subsurface ecosystems, causing negative effects on health, including birth deformities, neurological diseases, numerous malignancies and infertility impacting various organs.<sup>2</sup> The discharge of radioactive waste from Japan in August 2023 intensified this harm. Significant amounts of radionuclides are emitted into the surrounding environment

and disseminated globally *via* the hydrological cycle, presenting a substantial risk to Earth's ecology and human health. Storing radioactive wastewater for a decade prior to disposal can diminish the concentration of radionuclides with half-lives of less than two years (54Mn, 89Sr, 106Ru, 106Rh, and 134Cs) by over 96%. Nevertheless, following treatment with ALPS, nuclear wastewater continues to contain radionuclides with extended half-lives, including <sup>3</sup>H ( $t_{1/2} = 12.3$  years), <sup>14</sup>C ( $t_{1/2} = 5730$  years), <sup>60</sup>Co ( $t_{1/2} = 5.26$  years), <sup>90</sup>Sr ( $t_{1/2} = 28.79$  years), <sup>125</sup>Sb ( $t_{1/2} = 2.71$  years), <sup>129</sup>I ( $t_{1/2} = 1.57 \times 10^7$  years), and <sup>137</sup>Cs ( $t_{1/2} = 30.2$  years), among others.<sup>3</sup> Consequently, it is essential to devise sophisticated, efficient, and environmentally responsible solutions for the effective elimination of radionuclides to mitigate the potential dangers.

Currently, radioactive wastewater is purified using various procedures, such as ion exchange,<sup>4</sup> chemical precipitation,<sup>5</sup> bioprocesses,<sup>6</sup> adsorption,<sup>7</sup> evaporation and concentration,<sup>8</sup> and membrane separation techniques.<sup>9</sup> Adsorption has emerged as the primary approach for removing radioactive ions from wastewater because of its accessibility, efficacy, maturity, and ecological compatibility.<sup>10</sup> Numerous adsorbents have been utilized to remove radioactive ions, including covalent organic frameworks (COFs), multi-walled carbon nanotubes (MWCNTs), and clay materials.<sup>11–13</sup> However, these adsorbents

<sup>a</sup>State Key Laboratory of Efficient Utilization of Arable Land in China (Institute of Agricultural Resources and Regional Planning), Chinese Academy of Agricultural Sciences, Beijing 100081, China. E-mail: zhangqianru@caas.cn

<sup>b</sup>Division of Environmental Science and Ecological Engineering, Korea University, Seoul 02841, Republic of Korea

<sup>c</sup>College of Information Science and Technology, Dalian Maritime University, 1 Linghai Road, Dalian 116026, China. E-mail: jqliu@dlmu.edu.cn

<sup>d</sup>Chinese Academy of Fishery Sciences, Beijing 100141, China



are often expensive, complex to produce, have low yields, and have limited adsorption capacities. Thus, it is essential to create affordable and effective materials for radioactive ion removal applications.

In recent decades, metal-organic frameworks (MOFs) have emerged as an innovative type of porous solid material in the field of separation science.<sup>14</sup> MOFs, whose basic composition comprises metal centers interconnected by ligand bonds, have been recognized as promising candidates for the elimination of radioactive ions by adsorption owing to their good thermal and elastic properties, superior framework adaptability, and respiratory behavior.<sup>15</sup> For instance, MIL series MOFs are commonly used for the capture of U(vi).<sup>16</sup> Many researchers have created MOF derivatives with improved selectivity and adsorption capabilities by incorporating new components or functional groups into the MOF framework. Wang *et al.* developed an original MOF product, MIL-100(Fe)-DMA, utilizing a solvothermal technique for the effective removal of Sr<sup>2+</sup> and Cs<sup>+</sup> from radioactive wastewater.<sup>17</sup> Characterization, along with density functional (DFT) computations, identified that the unsaturated carboxylic acid groups on the MOF surface play an important role in interacting with Cs<sup>+</sup> and Sr<sup>2+</sup>. Zhang *et al.* employed ZIF-67 to laminate 2D MXene Ti<sub>3</sub>C<sub>2</sub> to increase the adsorption of radiocaesium from nuclear waste.<sup>18</sup> ZIF-67's laminating and columnar effects boosted Ti<sub>3</sub>C<sub>2</sub>'s specific surface area and interlayer spacing, which improved Cs<sup>+</sup> adsorption. The MXene lattice provided the primary adsorption sites and interactions that stabilized Cs<sup>+</sup>, whereas hybridized ZIF-67 facilitated loading. The fundamental theories and applications of MOFs have been thoroughly studied, covering their physicochemical properties, synthesis, and applications,<sup>19</sup> with their applications focusing on the study of volatile organic compounds, hazardous organic pollutants, heavy metal ions, and gases.<sup>20-22</sup> Unlike conventional contaminants, the design of radionuclide removal products must consider the following characteristics: (i) severe conditions, including highly acidic environments, increased significant ionizing radiation, and ionic strength; (ii) the influence of material characteristics on nuclear extraction (hydrophilicity, functional groups, electrostatic interactions, complexation, and polarity); (iii) the resilience and reusability of the adsorbents; (iv) the risk of contamination afterward; (v) economic implications and viability; and (vi) obstacles in adsorbent reprocessing.

Utilizing worldwide datasets to compare the findings of diverse studies presents a valuable chance to enhance our comprehension of the adsorption capability of MOFs and their derivatives concerning radioactive ions. In this research, we employed a meta-analysis to examine the effect of MOF materials on the loading performance of radioactive ions under various influencing circumstances to mitigate environmental contamination. A meta-analysis is a statistical procedure that assesses the impact of an unrelated variable on a dependent variable by synthesizing data from various scientific studies.<sup>23</sup> A key benefit of meta-analysis is its superior statistical power, yielding more reliable estimates than singular investigations.<sup>24</sup> To our knowledge, this is the first meta-analysis on this subject. The results of this study will yield novel perspectives on the

relationships between MOFs and radioactive elements, aiding decision-making for safeguarding the environment and handling risks in a dynamic context. The explicit objectives of this study are as follows: (1) to examine the multiple kinds and features of radioactive elements and MOFs, along with the effect of metal conditions on the adsorption behaviors of radioactive elements on MOFs; (2) to ascertain the key parameters influencing the loading of radioactive elements on MOFs and to forecast their loading performance; and (3) to elucidate the principal interaction mechanisms and contributing factors.

## 2. Methodology

### 2.1. Methodology for data acquisition and retrieval

The research program is based on a meta-analysis and systematic review conducted in accordance with the PRISMA criteria. This study aimed to investigate the extraction of radioactive elements from aqueous solutions containing metal-organic framework (MOF) particles. Articles were selected from 2016 to 2025. A thorough examination of the literature in the Web of Science core database was performed employing the following search equation: TS = (MOF\* OR metal organic framework\* OR MOF derivatives OR MOF composites OR modified MOF) AND TS = (radioactive element OR nuclear wastewater OR radioactive) AND TS = (adsorption OR removal).

### 2.2. Inclusion criteria

The inclusion criteria for this investigation comprised original English literature that employed MOFs for the extraction of radioactive elements from water-based solutions, either autonomously or in combination with other substances.

Publications under consideration must fulfill the following criteria: (1) the study must identify the specific type of MOF and radioactive ions utilized; (2) it should encompass measurements derived from at least three replicate property tests; (3) information regarding the adsorption of radioactive ions by the MOF must, at a minimum, include the quantity of adsorbed ions; and (4) the study must illustrate an initial or equilibrium concentration of the radioactive ions alongside an adsorbent dosage of the MOF.

According to the aforementioned criteria, 521 publications were selected, resulting in 25 articles remaining after applying the exclusion criteria (Table S2).

### 2.3. Data extraction and grouping

The investigations encompassed six types of radioactive elements (U, I, Cs, Sr, Tc and Re) and four categories of MOFs (pristine, metal-doped and ligand-modified MOFs, and MOF complexes). The data collected for each study included the main parameters for the preparation of MOFs and their derivatives (synthetic temperature, synthetic time, activation temperature, activation time, synthesis method, and eluent), batch experimental conditions (initial concentration, pH, equilibration time, and adsorbent dosage), modification strategies (metal doping, functional group modification, linkage complexes, and carbonation), and repetitive experimental conditions (eluent,

number of replicates, and adsorption decrease rate). Data were obtained from the diagrams *via* GetData Graph Digitizer (version 2.24).

The metal centers of MOFs are divided into two groups: (1) low valence metals such as Cu, Bi, Ag, Cd, Zn, Co, and Pd, and (2) high valence metals such as Fe, Zr, Al, In, and Ce. Among the radioactive elements,  $\text{Sr}^{2+}$  and  $\text{Cs}^+$  are metal cations,  $\text{I}_2$  is a molecule, and  $\text{UO}_2^{2+}$  and  $\text{TeO}_4^-/\text{ReO}_4^-$  are metal oxygen cations. The synthesis/activation temperatures were categorized as hypothermy ( $<100$  °C), mesotherm (100–120 °C) and hyperthermia ( $>120$  °C). The equilibrium/activation time was divided into fast ( $<12$  h), medium (12–24 h) and slow ( $>24$  h). The initial concentration was categorized as low ( $<500$  mg L $^{-1}$ ), medium (500–1000 mg L $^{-1}$ ) and high ( $>1000$  mg L $^{-1}$ ). Dosage was categorized as low ( $<0.1$  g g $^{-1}$ ), medium (0.1–1 g g $^{-1}$ ), and high ( $>1$  g g $^{-1}$ ). The equilibration time was categorized as fast ( $<1$  h), medium (1–6 h) and slow ( $>6$  h). The pH was categorized as alkaline ( $>8$ ), neutral (6–8) and acidic ( $<6$ ).

#### 2.4. Statistical analysis of data

The natural logarithm of the response ratio ( $\ln \text{RR}$ ) was used to determine the effect of each component on the removal of radioactive ions from the MOFs. The natural logarithm of the risk ratio ( $\ln \text{RR}$ ) was selected as the effect size (ES) due to the unbiased computation despite variations in the sample sizes between treatments.<sup>25</sup> Calculations were performed using the following equation:

$$\text{ES} = \ln\left(\frac{X_e}{X_c}\right) \quad (1)$$

where  $X_e$  denotes the concentration of radioactive ions after adsorption by the MOF and  $X_c$  represents the initial concentration of radioactive ions before loading (mg L $^{-1}$ ). A low level of ES signifies elevated quantities of radioactive ions loaded onto microplastics.

Heterogeneity among several categories of  $\ln \text{RR}$  was assessed utilizing the 95% confidence interval (95% CI) within the framework of the uncontrolled effect model.<sup>26</sup> A 95% confidence interval that is evenly distributed with 0 signifies a substantial reaction to the interaction.<sup>27,28</sup> The details are provided in the SI.

#### 2.5. DFT computational methods

In this study, geometry optimization and vibration frequency calculation with empirical dispersion correction were performed using GB3LYP/Def2-SVP through the BDF module of Device Studio software.<sup>29–31</sup> In this study, representative original MOFs from 25 screened papers were selected, and CIF files were acquired from the Cambridge Crystallographic Data Center (CCDC). Considering the periodicity of the MOFs, a single nucleotide cluster model with a metal as the node and carboxyl groups on the surface was chosen to improve the computational efficiency. Considering the solvation effect in water ( $\epsilon = 78.35$ ), the SMD implicit solvation method was used, and the optimized geometries obtained from vacuum calculations were used as starting geometries for additional calculations. Surface

electrostatic potentials (ESPs) were computed utilizing Multifn\_3.8.<sup>32,33</sup> All images were created using VMD 1.9.3.<sup>34,35</sup>

## 3. Results and discussion

### 3.1. The importance of structural stability in MOFs

MOFs possess isolated metal sites and reticulated chemical structures featuring distinct molecular secondary building blocks that can dictate orientation.<sup>36</sup> The modular characteristics of MOFs facilitate their assembly by integrating various organic linkers, inorganic components, and topologies while ensuring the preservation of structural integrity and porosity at high temperatures or in liquid environments, to be effectively utilized as catalysts or functional materials. For utilization as catalysts or functional materials, MOFs must preserve their structural integrity and porosity under elevated temperatures or in liquid phase environments.

In general, highly stable MOFs can be attained by enhancing the binding strength between organic ligands and metal nodes.<sup>37,38</sup> This implies that stable MOFs are formed *via* hydrophobic pores, including ZIF-67 and ZIF-8, which shield metal-ligand linkages from water molecules.<sup>39</sup> This can produce stable MOFs using HASB theory. Fig. S2b depicts the main principles for selecting the metals and ligands needed to create stable MOFs using HASB theory.<sup>40</sup> Stable MOFs have been synthesized using high-valence metal ions such as  $\text{Cr}^{3+}$ ,  $\text{Zr}^{4+}$ , and  $\text{Fe}^{3+}$  with carboxylate-type ligands. The high quantity of high-priced metal units with better coordination in MIL-101(Cr), UiO-66 (Zr), and MIL-100(Fe) often results in a very stiff structure, making the metal sites less sensitive to water molecules and offering good water stability.<sup>41–43</sup> MIL-53 and UiO-66 preserved their crystalline forms in air at temperatures of 500 °C and 400 °C, respectively.<sup>44</sup> Another technique for the production of stable MOFs is the use of azolate-containing ligands (including pyrazole, imidazole, tetrazole, and triazole) to bind with divalent metal ions. The most prominent MOF of this category is the zeolite imidazole salt skeleton (ZIFs), which uses  $\text{Zn}^{2+}/\text{Co}^{2+}$  and imidazole salt connectors to build diverse stable crystals with topologies comparable to those of zeolites.<sup>45,46</sup> The number of research articles on the stabilization of metal-organic frameworks (MOFs) is currently increasing, with a growing number of stabilization MOFs published annually, attributed to enhanced understanding of their structural stability in aqueous environments and ongoing efforts. Several stable MOFs are shown in Fig. S2c.

Furthermore, MOFs can be precisely modified to achieve spatial site resistance, thus maintaining their robustness in aqueous media.<sup>37,38</sup> Hydrophobic porous surfaces or encapsulated metallic ions may hinder water molecules from infiltrating the lattice and compromising the structural integrity. For example, hydroquinone electron transfer results in the reduction of copper ion coordination.  $\text{Cu}(\text{n})$  increases HKUST-1. Water molecules are prevented from attacking the metal coordination bonds by a specific node  $[\text{Cu}(\text{MeCN})_4]^+$  produced by the interaction of free  $\text{Cu}^+$  with the MeCN solvent.<sup>47</sup> Taylor *et al.* demonstrated that the CALF-25 structure's non-polar alkyl functional groups permit it to load huge volumes of liquid



medium while remaining stable owing to functional group shielding around the metal core.<sup>48</sup> Durable superhydrophobic/superoleophilic polyurethane (PU) sponges, synthesized through the self-polymerization of dopamine and chemical modification of low-surface-energy components to functionalize UiO-66-(COOH)<sub>2</sub>, demonstrate exceptional chemical, thermal, and mechanical resilience when subjected to corrosive mixtures, boiling water, and sandpaper abrasion tests.<sup>49</sup> Fluorinated MOF-808-PFOA was prepared *via* substituting the acetic acid in MOF-808 with pentadecafluoroctanoic acid (PFOA), and thus submicron MOF-808-PFOA was incorporated into melamine (MA) sponges using the cross-linking properties of polydimethylsiloxane (PDMS). The MOF/PDMS/MA sponge exhibited a significant contact angle of 151.9°. Superior hydrophobicity was preserved across a broad spectrum of aquatic environments and pH levels. The sponge demonstrates exceptional adsorption capabilities for diverse organic oils due to its strong hydrophobicity, mechanical durability, and porous structure, with a substantial saturation adsorption capacity (27–65 g g<sup>-1</sup>), rapid equilibration time (approximately 3 s), and commendable recoverability.<sup>50</sup>

The screening of MOFs predominantly depends on expert intuition to select potential materials for subsequent syntheses. Numerous exceptions exist regarding the predictions for metal joint bond strengths in relation to MOF stability, which constrain the general use of heuristics for stability forecasting. Density Functional Theory (DFT) is a fundamental method for forecasting novel hypothetical structures and their characteristics and computing energy band structures, excitation energies, and densities of states. It has been effectively utilized in Metal–Organic Frameworks (MOFs).<sup>51,52</sup> DFT calculations are generally applicable to small molecules and periodic crystals. Molecular modeling techniques have been effectively utilized for simulations, predictions, and computational characterization of MOF structures, along with complicated structure determination, encompassing assumptions regarding the large-scale screening and geometric characteristics of MOFs.<sup>53</sup> Computational studies utilizing DFT have been employed to ascertain the structure of MOFs and their complexes, predict properties, and conduct computational characterization of MOFs, encompassing geometrical properties, massive screening assumptions, and diffusion and loading procedures

within MOFs. DFT computations have been utilized in the domain of MOFs to investigate features, including chemical stability. This study examined the stability of eight pristine metal–organic frameworks (MOFs) derived from twenty-five publications. The relevant crystal CIF files were obtained from the Cambridge Structural Database (CSD).

DFT calculations were performed to evaluate the influence of aqueous solvents on MOFs. Quantitative molecular surface analysis facilitates the examination of the distribution of the electrostatic potential (ESP) on the van der Waals surface of a molecule. The application of molecular volume, surface area, and diverse metrics derived based on the spatial distribution of ESP on the surface of a molecule (collectively termed GIPF descriptors), including the extreme values of the electrostatic potential, its variance, and mean, can be employed to forecast the properties of a molecule's cohesive phase (Fig. 1). The equation for forecasting the hydration free energy (solvation free energy) of molecules in an aqueous environment was proposed as early as 1999 (ref. 54) as follows:

$$\Delta G_{\text{solve}}(\text{kJ mol}^{-1}) = 0.17201 V_m - 2.6414 \times 10^{-5} (V_{S,\text{max}} - V_{S,\text{min}})^3 + 0.051892 A^- \bar{V} \bar{s} + \frac{9704.2}{A^- \bar{V} \bar{s}} + 46.827$$

The molecular volume,  $V_m$ , represents the minimum ESP throughout the three-dimensional space, while  $V_{S,\text{min}}$  and  $V_{S,\text{max}}$  denote the minimum and maximum ESP values on the surface of the molecule, respectively.  $A^-$  denotes the surface area of the region, where the ESP on the surface of the molecule is negative, while  $\bar{V} \bar{s}$  represents the average electrostatic potential in the area where the potential on the static molecule's surface is negative.

These data are shown in Table S1. The hydration free energies predicted according to this method differed from the hydration free energy calculated *via* the implicit solvent model by only 0.01–0.02 au. The affinities of the MOFs for the aqueous solvents were calculated based on the calculated values of the hydration free energy (Table S1). The solvation free energies showed that among the five MOFs, the order of affinity to solvent water was as follows: CAU-17 > MOF-303 > ZIF-90 > MIL-53 > ZIF-8.

Despite their outstanding water stability and tremendous potential in radioactive ion restoration applications, their

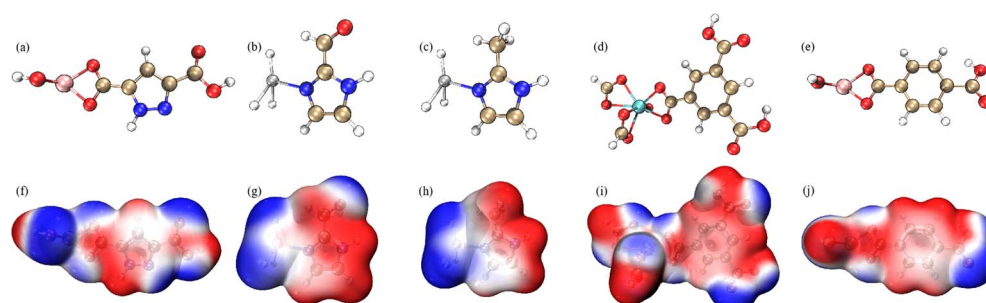


Fig. 1 Geometry of (a) MOF-303, (b) ZIF-90, (c) ZIF-8, (d) CAU-17, and (e) MIL-53 and surface electrostatic potential of (f) MOF-303, (g) ZIF-90, (h) ZIF-8, (i) CAU-17, and (j) MIL-53.



resilience to ionizing radiation has not been well documented. Among the 25 studies reviewed in this study, only one examined the stability of MOFs under  $\beta$ -radiation exposure.<sup>55</sup> The experimental results indicate that the powder XRD spectra of MOF-303 samples subjected to different  $\beta$ -ray irradiation dosages align closely with the powder XRD spectra of the original MOF-303. The full width at half height (FWHM) measurements exhibited slight fluctuations with increasing irradiation dose, indicating that the crystallinity remained mostly intact. This phenomenon can be substantiated by the adsorption–desorption isotherm at 277 K, predicated on the nitrogen-based pore characteristics. After irradiation, the specific surface area was marginally reduced or similar to that of pristine MOF-303. The FTIR and XPS spectra exhibited no notable changes before and after irradiation. The authors determined that the MOF-303 structure exhibited considerable stability during  $\beta$ -irradiation, even at 1000 kGy. Such consistency can be ascribed to the following variables: (i) Al, the metal center of MOF-303, possesses an unchanged valence state and a generally stable coordinating mode; and (ii) Al has a minimal metal cross-sectional region, reducing the interaction region with electron beam radiation and consequently mitigating the significant damage caused by radiation.

The mechanism underlying the reactivity of MOFs to gamma radiation remains ambiguous; however, there are indications as to why one material exhibits greater stability than another. Gamma rays interact with matter through three primary processes: the Compton effect, photoelectric effect, and pair production. The probability of such reactions is significantly dependent on the energy of the gamma rays and the atomic number ( $Z$ ).<sup>56</sup> The dominance of the Compton consequence is anticipated based on the gamma energies of the elements constituting the MOF ( $E_\gamma = 1.17$  and 1.33 MeV) and  $Z$  values. The Compton procedure comprises a portion of the transmission of energy to electrons throughout the MOF, which leads to the loss of energy of gamma radiation that can subsequently contact other electrons, leading to a secondary photoelectric effect or Compton impact, producing recoil electrons. Certain Compton electrons may traverse air without colliding, whereas others may interact with the orbital electrons of adjacent atoms in the MOF *via* incoherent scattering, resulting in ionization or excitation. Ultimately, the energy of the excited atoms can be released *via* the release of orbital electrons or fluorescence, which may subsequently be wasted as vibrational energy (heat). The structure of a MOF influences its resistance to radioactivity. The mass–energy coefficient for adsorption quantifies the mean proportion of photon energy captured by a substance. The metal clusters in the MOFs examined in the present study comprised oxygen and metal atoms, and their overall attenuation coefficients significantly exceeded those of the organic connectors, indicating that the metal clusters may function as radiating antennas. The aromaticity of organic linkers significantly influences the stability of MOFs in a  $\gamma$ -ray environment. These flaws may hinder energy transfer and dissipation, leading to a diminished tolerance of MOFs to  $\gamma$ -radiation.

Nonetheless, as radiation procedures may expedite production and provoke diverse chemical processes, irradiation

technology has increasingly been employed as an innovative and efficient approach for preparing and altering the chemical and physical properties of MOFs, including gamma-ray ( $\gamma$ -ray) radiation. Gamma-ray radiation is often generated by the emission of photons with limited wavelengths and elevated energy during the radioactive disintegration of atomic nuclei. It has significant penetration capability, resulting in irreversible structural alterations.<sup>57</sup> Recent research indicates that metal–organic frameworks (MOFs) are essential in nuclear energy applications because of their high capacity and selectivity for radionuclide adsorption. Marinkovic and colleagues<sup>58</sup> exhibited the impact of  $\gamma$ -ray radiation on the dielectric characteristics of LDPE/ZIF-8 composites. The composites demonstrated enhanced conductivity with increasing  $\gamma$ -ray dose. Nonetheless, ZIF-8 deteriorated with escalating  $\gamma$ -ray exposure, leading to a reduction in conductivity above a specific radiation dose threshold. Lafi and colleagues<sup>59</sup> noted enhanced iodine adsorption following the  $\gamma$ -ray irradiation treatment of MIL101 (Cr) at optimal dosages of up to 15 kGy. Primarily,  $\gamma$ -ray radiation significantly influences the framework and characteristics of MOFs. To date, most research has focused on the alterations in the adsorption characteristics and irradiation stability of MOFs subjected to  $\gamma$ -ray radiation. According to reports, different linker connections and metal loadings influence the radiative stability of metal–organic frameworks (MOFs), whereas structural modifications produced by  $\gamma$ -rays affect their conductivity and adsorption characteristics.

### 3.2. Parameters influencing capacity for adsorption

**3.2.1 Impact of MOF synthesis methods on adsorption capacity.** This section examines the impact of several MOF synthesis methods on the loading capacity of radioactive ions. The synthesis parameters include the metal source type, synthesis temperature, synthesis time, synthesis type, activation temperature, and activation time. Alterations in each of the above variables may result in modifications to loading performance. In the case of the capture of U(vi), for the MOF metal source valence type, the adsorption capacity effect of the high-valent metal source (0.76, 95%CI = 0.65, 0.85,  $P < 0.05$ ) was significantly greater than that of the low-valent metal source (0.46, 95%CI = 0.35, 0.57,  $P < 0.05$ ). This disparity may be due to the original MOF species identified in the 25 selected studies, which conform to the structure of metal–oxygen clusters. According to HSAB theory, core atoms that are diminutive, possess a high positive charge, and exhibit limited polarizability are classified as hard acids, making them compatible with electronegative species. It is appropriate for amalgamating with ligand atoms that possess high electronegativity and low polarizability and are resistant to oxidation. The crystal structure was stable and maintained its integrity throughout the reaction process, effectively facilitating the stable coordination of U(vi). The adsorption capacity at varying synthesis temperatures was as follows: high temperature (0.79, 95% CI = 0.73, 0.86,  $P < 0.05$ ) > medium temperature (0.66, 95% CI = 0.48, 0.83,  $P < 0.05$ ) > low temperature (0.54, 95% CI = 0.45, 0.63,  $P < 0.05$ ). A thermal stability study of MOFs revealed that the bond energy



of the ligand bond between the organic ligand and metal is inferior to that of covalent and metal bonds. Additionally, frameworks with highly permeable structures inadequately support their own mass. Upon the removal of numerous free solvent molecules, these highly open frameworks exhibit significant torsion and deformation, resulting in a loss of crystallinity; some may even collapse, severely compromising the crystal structure of MOF materials and transforming them into amorphous powders. The thermal stability of MOFs can be markedly enhanced by elevating the synthesis temperature within a specific range. The same is true for the synthesis time, which can increase the adsorption capacity by extending the synthesis time to a certain extent. This argument is supported by the conclusion shown in Fig. 2. For the impact of synthesis techniques on ability to adsorb, microwave (0.88, 95%CI = 0.87, 0.88,  $P < 0.05$ ) > standing (0.84 95%CI = 0.73, 0.94,  $P < 0.05$ ) > solvothermal (0.52, 95%CI = 0.71, 0.73,  $P < 0.05$ ) > ultrasound (0.64 95%CI = 0.62, 0.64,  $P < 0.05$ ) > stirring (0.84 95%CI = 0.50, 0.54,  $P < 0.05$ ) in the 25 papers screened. Every approach possesses distinct advantages and limitations, and solvent heat is the most widely used method, followed by stirring, which is mostly used for the synthesis of ZIF-series MOFs at room temperature. Among the many methods for MOF synthesis, the microwave method is novel. In microwave technology, the molecules within the microwave oscillate at a high frequency, resulting in the uniform heating of the components within the microwave vial during the reaction process. The constant elevation of reaction temperature enables MOFs to crystallize within minutes, much outpacing solvothermal techniques. Nonetheless, microwave synthesis has challenges in producing sufficiently large crystals for single-crystal X-ray characterization and may be less suitable for industrial uses. The produced MOFs are predominantly encased by solvents and unreacted precursors that may occupy the pores, necessitating the removal of undesirable substances through a process known as

activation. The elimination of solvent molecules, particularly those with elevated boiling points or high surface tension, can result in structural collapse because of the significant surface tension and capillary forces produced on the framework during the process in which the entrapped solvent molecules change from liquid to gas. The effects of activation duration and temperature on the adsorption capacity are essential. The breakdown temperature of the MOF was established from the thermogravimetric (TGA) curve, and the MOF was subsequently heated to a temperature that was half of the decomposition temperature to effectively eliminate small guest molecules (e.g., methanol and ethanol) from the MOF.

In the adsorption process of Sr and Cs, the effect of the amount of high-valence metal source with a high synthesis temperature was the highest in terms of metal source type and synthesis temperature type (Fig. 3). The effect size of solvation was higher than that of stirring, and the effect size of activation temperature did not satisfy the proportional relationship between temperature and adsorption, which may be because, at high activation temperatures, the MOF structure was decomposed, and the instability of the structure negatively affected the adsorption capacity.

**3.2.2 Influence of experimental parameters on loading capacity.** This section examines the implications of various experimental settings on the ability to adsorb radioactive ions (Fig. 4 and 5). The experimental conditions included the original concentration of the radioactive ion solution, pH, reaction time, and adsorbent dose. Changes in any of these factors may result in changes in the adsorption capacity. The trends in the effect magnitudes of uranium, strontium, cesium, and thorium under varying conditions were nearly identical, with the effect magnitudes of strontium, cesium, and thorium increasing as the initial concentration of radioactive ions increased. This suggests that, within this range of initial concentrations, the active sites of the MOF are not fully occupied by radioactive ions

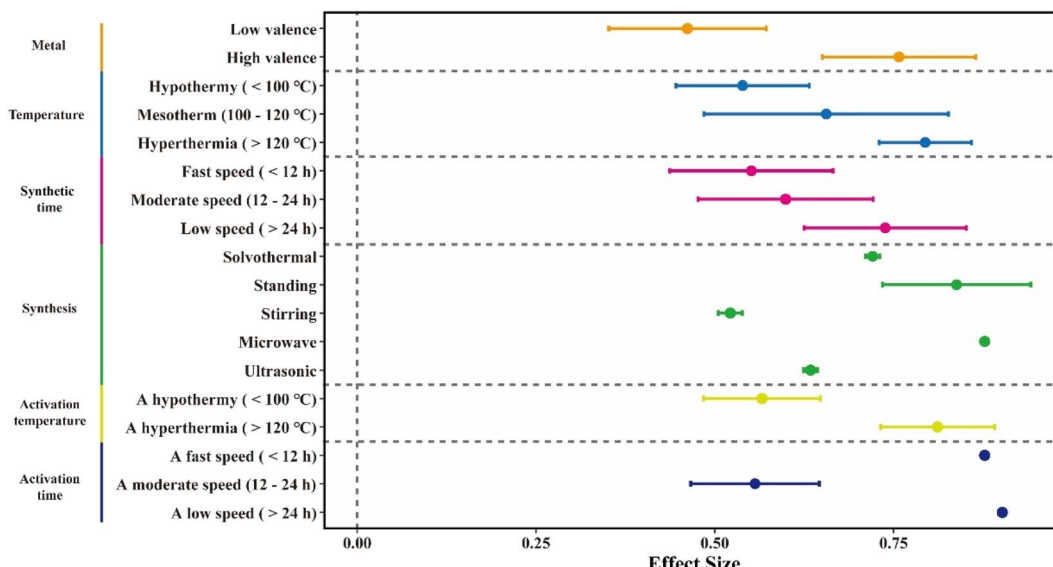


Fig. 2 Effect of synthesis conditions on uranium adsorption capacity. Horizontal error lines indicate 95% confidence intervals.



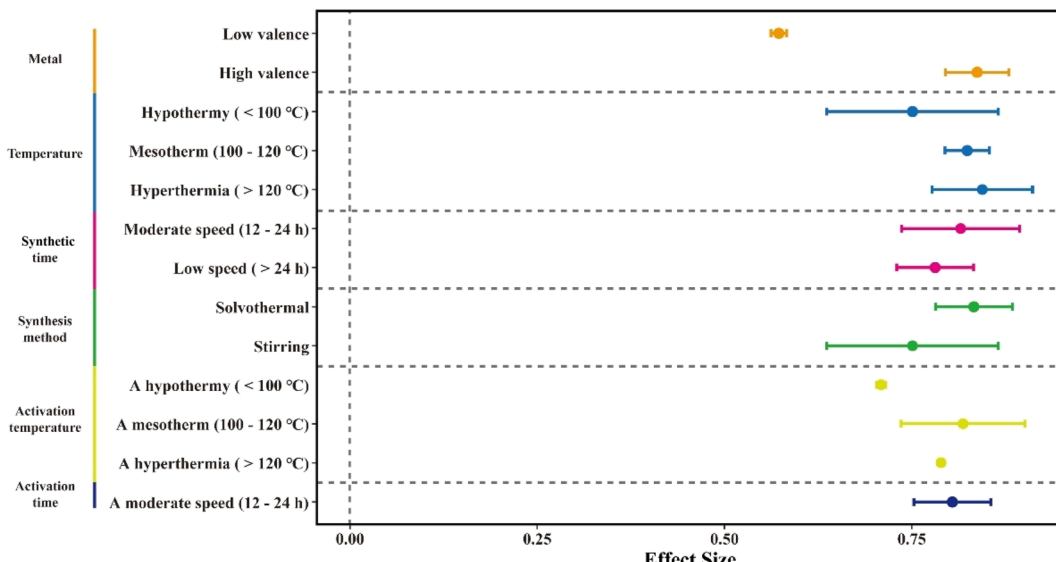


Fig. 3 Impact of synthesis conditions on the loading performance of strontium cesium thorium. Horizontal error lines indicate 95% confidence intervals.

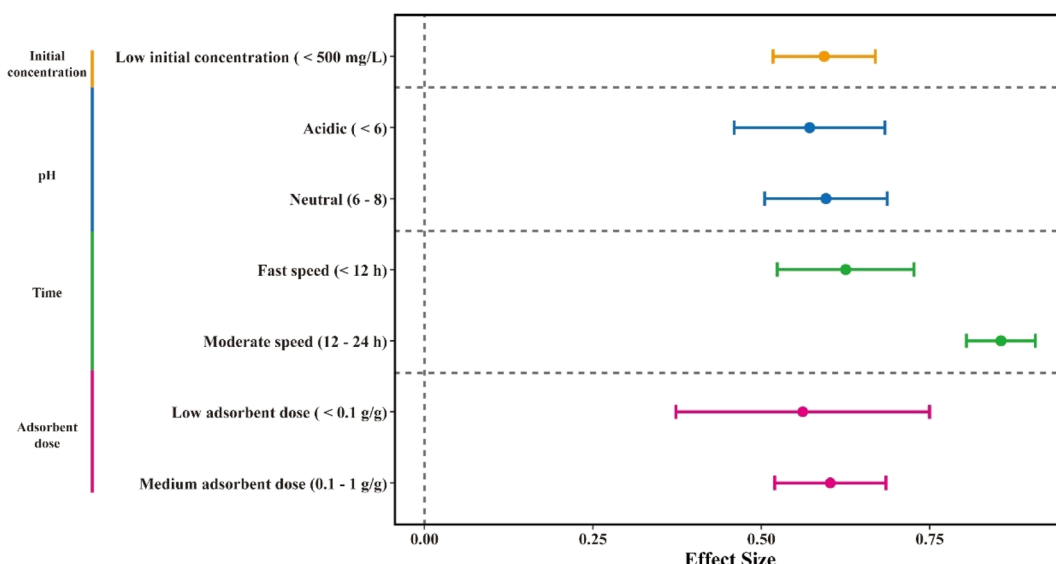


Fig. 4 Impact of experimental conditions on the capture performance of uranium-thorium. Horizontal error lines indicate 95% confidence intervals.

and the reaction has not yet attained equilibrium. The optimal effect for uranium, strontium, cesium, and thorium occurred within the pH range of 6–8, as it was posited that the metal-organic framework (MOF) would deteriorate under acidic or alkaline conditions, leading to structural degradation and a marked reduction in MOF stability. However, this study discusses the adsorption of radioactive ions by MOFs, while extreme pH conditions prevail in nuclear wastewater, and it is evident that there is still a long way to go in the treatment of nuclear wastewater using MOF materials. The adsorbent dose significantly affects the uptake performance of MOFs for radioactive ions. The effect of  $\text{UO}_2^{2+}$  at a medium adsorbent

dose exceeds that at a low adsorbent dose, which aligns with the conclusion that the adsorption capacity stabilizes with increasing adsorbent dose once a specific threshold is attained, as evidenced by numerous experiments.

The rate of rapid adsorption of radioactive ions by MOF materials is influenced by multiple factors, among which the intrinsic properties of the materials are fundamental. Particle size and pore size are key structural factors: smaller particles shorten the diffusion path, increase site accessibility, and accelerate adsorption (especially in the initial stage); however, if too small, they tend to aggregate and clog the pores. Larger particles have slower diffusion and fewer accessible sites. The



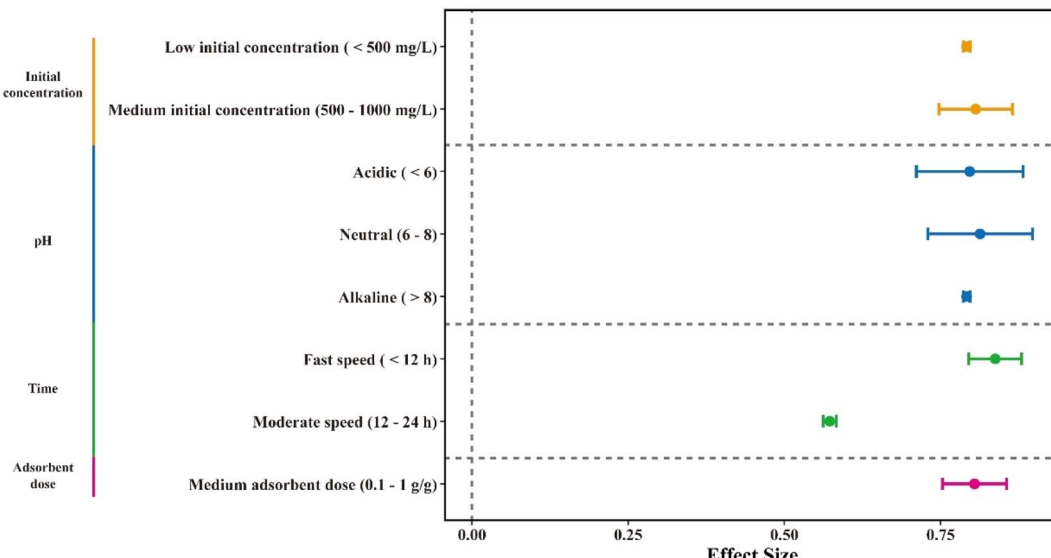


Fig. 5 Impact of experimental conditions on the uptake capacity of strontium cesium thorium. Horizontal error lines indicate 95% confidence intervals.

pore size should be slightly larger than the hydrated diameter of the target ions (e.g.,  $\text{UO}_2^{2+}$  is about 0.8 nm and  $\text{Sr}^{2+}$  is about 1.18 nm) to ensure free entry of ions and efficient binding to sites – too small will cause steric hindrance, while too large will reduce the site density and driving force. The introduction of a hierarchical pore structure (micro-pores + meso-pores) can synergistically optimize diffusion and adsorption. Additionally, the functional groups on the pore inner walls must balance the selectivity and pore size effectiveness.

However, as shown in Table S4, the particle and pore sizes are not decisive factors. The chemical nature of the surface functional groups of MOFs (such as carboxyl and amino groups) and the surface charge state (regulated by pH) directly determine the interaction mechanism with ions (such as coordination and electrostatic attraction). The structural stability of MOFs in water environments is crucial; structural collapse significantly reduces the number of effective adsorption sites and severely lowers the adsorption rate.

**3.2.3 Effects of modification strategies on MOF properties and adsorption capacity.** Emerging MOFs present opportunities for improved and sustainable water repair techniques. Consequently, water pollution treatment technology has progressed from ‘functional and precise’ materials to ‘functional, precise, and designable’ materials. The composition and characteristics of MOFs can be modified using various methods, including acid regulation, modification with different functional groups, noble metal loading, and other methods.<sup>57</sup>

Post-synthetic modifications have demonstrated significant potential for methodically modifying the structures of MOFs and enabling the creation of functional MOFs that are not synthesized directly. PSM methodologies for the functionalization of MOFs can be categorized into three principal types: functional organic linkers, metal sources, and noncovalent encapsulation.<sup>60</sup> The initial two tactics are the most appealing.

The incorporation of an organic molecule that establishes a metal site with an unsaturated molecule to create coordination bonds in MOF secondary building units (SBUs) is feasible, particularly in the absence of linker defects, surface sites, low-nucleation clusters, or, in certain circumstances, the total replacement of the original linker. Functional groups ( $-\text{COOH}$ ,  $-\text{NH}_2$ ,  $-\text{NO}_2$ ,  $-\text{OH}$ ,  $-\text{SH}$ , etc.) were incorporated into the designated MOFs by sequentially attaching organic compounds. The findings indicated an increase in the number of active adsorption sites and the selectivity of the pristine MOFs. Furthermore, metals were incorporated into the MOF structures and affixed to the connections by ligand bonding. Various MOF structures have demonstrated the ability to release co-ligands under specific conditions, enabling the utilization of unsaturated metal clusters for additional functionalization. Functional groups such as amide, phosphorylurea,<sup>61</sup> amidoxime,<sup>62</sup> carboxyl, sulfate,<sup>63</sup> and ferricyanide<sup>64</sup> groups play an essential role in the loading of radioactive ions. Functionalized MOFs have the characteristics of both MOFs and the additional groups and have obvious selectivity for radioactive ions, thus greatly improving the adsorption capacity of the material. A novel MIL-100(Fe)-DMA material was manufactured using a solvothermal technique.<sup>17</sup> The unsaturated carboxylic acid groups of MIL-100(Fe)-DMA were critical in the adsorption process, and DFT calculations combined with experimental characterization revealed the adsorption behaviors of  $\text{Sr}^{2+}$  and  $\text{Cs}^+$  through MIL-100(Fe)-DMA. After capture, the framework structure and crystallinity of the material remained unchanged, implying that the radioactive ions  $\text{Sr}^{2+}$  and  $\text{Cs}^+$  had no major effect on the MOF structure. Sang *et al.* created a unique U(vi) adsorbent (ZIF-90-A) with anti-bio-contamination capabilities by post-modifying ZIF-90.<sup>62</sup> Experimental characterization verified that ZIF-90-A was highly effective in eliminating U(vi) at pH 5. ZIF-90-A demonstrated consistent antibacterial efficacy



against *Staphylococcus aureus* and *Escherichia coli* (MICs = 125–250  $\mu\text{g mL}^{-1}$ ) and exhibited exceptional adsorption capacity for  $\text{UO}_2^{2+}$  ( $Q_e = 490.2 \text{ mg g}^{-1}$ ). ZIF-90-A demonstrated consistent antibacterial efficacy against *Staphylococcus aureus* and *Escherichia coli* (MICs = 125–250  $\mu\text{g mL}^{-1}$ ), as well as notable selectivity and superior adsorption characteristics for  $\text{UO}_2^{2+}$ . Furthermore, the synthesized adsorbent demonstrated significant selectivity and outstanding restoration for  $\text{UO}_2^{2+}$  ions. The primary processes of  $\text{UO}_2^{2+}$  adsorption are chemical coordination and electrostatic contact. Lin *et al.* documented the effective capture of  $\text{Sr}^{2+}$  in a stabilized two-group Zr-BDC-COOH-SO<sub>4</sub> with strontium-chelating groups (-COOH and -SO<sub>4</sub>) and a significantly ionizing group (-COOH).<sup>63</sup> Zr-BDC-COOH-SO<sub>4</sub> demonstrates a maximal adsorption capacity of 67.5 mg g<sup>-1</sup> and rapid adsorption kinetics (<5 min). Subsequent investigations indicated that the loading of  $\text{Sr}^{2+}$  onto Zr-BDC-COOH-SO<sub>4</sub> was not markedly influenced by the solution pH or the interaction temperature. Mechanistic investigations indicated that free -COOH facilitates quick adsorption through electrostatic interactions, whereas the incorporation of -SO<sub>4</sub> significantly increases the adsorption capacity. Le *et al.* prepared a new ZIF-8-FC derivative, including ZIF-8 modified by FC, using a straightforward production approach at ambient temperature. The maximum loading content of ZIF-8 for Cs<sup>+</sup> was 26.54 mg g<sup>-1</sup>, whereas that of ZIF-8-FC for Cs<sup>+</sup> was 422.42 mg g<sup>-1</sup>.<sup>65</sup> ZIF-8-FC exhibited a  $K_d$  of  $5.3 \times 10^4 \text{ mL g}^{-1}$  in deionized water. The adsorption efficacy remained consistently steady across an extensive pH range.

Metal-doped MOF materials represent a contemporary trend designed to enhance the number of active sites in MOFs and expand their applicability. Researchers currently mix two or more metal ions to create homogeneous bimetallic or multi-metallic MOF materials, aiming to use the advantages of individual components *via* the coupling effect to attain certain performance outcomes. A complex adsorbent, Ca/Mg-MOF/polyamide oxime (Ca/Mg-MOF/PAO), was prepared and evaluated for its capacity to absorb uranium(vi) from a solution.<sup>66</sup> The composition and properties of Ca/Mg-MOF/PAO were also analyzed. Batch tests revealed that Ca/Mg-MOF/PAO demonstrated a remarkable saturation performance of 579.5 mg g<sup>-1</sup> for  $\text{UO}_2^{2+}$  at pH 8, exceeding those of numerous other adsorbed materials. UiO-66-NH<sub>2</sub>, a unique Ce/Mn bimetallic modified aminated MOF, was produced using a solvothermal reaction and utilized as an adsorbent in radioactive remediation.<sup>67</sup> The maximum uptake content of  $\text{UO}_2^{2+}$  through the synthesized adsorbent at 313 K was 1218.78 mg g<sup>-1</sup>, with a capture effectiveness of more than 83.5% after five regeneration cycles, demonstrating that Ce/Mn-UiO-66-NH<sub>2</sub> is a promising adsorbent for removing  $\text{UO}_2^{2+}$  from radioactive wastewater. The increased absorption capability is due to the complexation and electrostatic attraction of radioactive substances with additional functional groups, such as Ce<sup>3+</sup> or Mn<sup>2+</sup>.

In addition to the benefits of MOFs, which include an extensive specific surface area, elevated porosity, and adaptability, MOF composites are frequently integrated with various functional materials, such as graphene oxides, magnetic nanoparticles, nanoporous carbon, and ionic liquids, to

enhance their adsorption capacity. Guo *et al.* created a new SNU-6 modified with 200-crown-18 for extracting  $\text{Sr}^{2+}$  from an acidic feed mixture.<sup>46</sup> The adsorbent employs the pronounced  $\text{Sr}^{2+}$  selectivity of 18-crown ether, and its unique binding site generates a  $\text{Sr}^{2+}$  selective MOF. The cavity dimension of the crown ether aligns with the radius of  $\text{Sr}^{2+}$  to form a stable compound. The substance has a notable affinity for  $\text{Sr}^{2+}$  ( $K_d = 3.63 \times 10^4 \text{ mL g}^{-1}$ ) and demonstrates a substantial loading performance of 44.37 mg g<sup>-1</sup>. The material demonstrates enhanced selectivity relative to other coexisting ions that interfere including K<sup>+</sup>, Na<sup>+</sup>, Cs<sup>+</sup>, Ca<sup>2+</sup>, and Mg<sup>2+</sup>, which is mostly due to the characteristics of the crown ether ligands. Liu *et al.* utilized an *in situ* synthetic technique to fabricate AMP-modified UiO-66 composites as a novel material for the selective extraction of <sup>137</sup>Cs<sup>+</sup> from low-level liquid wastes (LLLWs).<sup>61</sup> UiO-66/AMP is appropriate for various Cs<sup>+</sup> aqueous solutions throughout the pH range of 4–11, demonstrating rapid adsorption kinetics and good selectivity for ppb-level concentrations of Cs<sup>+</sup>. The specific surface area of UiO-66/AMP was 29.07 m<sup>2</sup> g<sup>-1</sup>, which was markedly lower than that of the original MOF, which was 1042.05 m<sup>2</sup> g<sup>-1</sup>. At the final stage of synthesis, the surface pores of the MOF were occluded by phosphate impurities and AMP, causing a substantial reduction in the specific surface area because of partial degradation of the MOF.

The synthesis of porous functional carbon materials using high-temperature carbonization with metal-organic frameworks as templates has emerged as a prominent research focus.<sup>68</sup> The PCs derived from the mechanical carbonization of the MOF exhibited enhanced chemical stability while retaining the systematically ordered pore structure of the MOF. Nonetheless, a noteworthy barrier to the utilization of porous MOF-derived carbon materials is their typical form as particles or crystals with small particle sizes, complicating their immobilization and separation in adsorption tests. A viable approach to mitigating these limitations is to immobilize metal-organic frameworks (MOFs) with other materials that exhibit superior polymerization properties, such as polyaniline compound carbon aerogels, carbon nanotubes, and graphene.<sup>69</sup>

Programmable pathways can significantly enhance the functional complexity and structure of MOFs through these composite techniques. The functionalization or derivatization of MOFs as precursors enhances the potential of lattice-based material design. Consequently, they can offer numerous alternative matrices for water pollution remediation.

### 3.3. Limitations of MOF materials for nuclear wastewater applications

#### 3.3.1 Summary of the commercial value of MOFs.

MOFs present virtually infinite combinatorial options, with over 14 000 MOFs synthesized to date. A unique MOF can be customized for a particular problem or application. The drawback of this distinctive material design method is the difficulty in attaining economies of scale with a singular MOF. Consequently, MOFs will continue to be more expensive than traditional adsorbents such as zeolites and carbon, at least in the

near future. MOFs are well positioned in the short to medium term to address challenges that current technologies cannot resolve or are too costly, provided that the incremental expense is justified by the resultant performance advantages. The commercial production of MOFs has accelerated consistently. Ohara Paragium Chemical is a Japanese firm specializing in the production of rapid deodorants. The company's Porous Coordination Polymer/Metal Organic Frameworks (PCP/MOF) were subsequently granulated with activated carbon to produce the inaugural commercial granular products in Japan. One gram of PCPMOF has a specific surface area equivalent to approximately 27 tennis courts, significantly exceeding the surface area of two tennis courts for the same mass of activated carbon. Moreover, MOF WORX utilizes the flow synthesis method to incrementally scale the laboratory-grade 10 mL reactor to a 1.394 L reactor for the large-scale production of MOF powder. Daily production may surpass 80 000 kg m<sup>-3</sup> when the reaction temperature and flow rate are meticulously regulated. The available MOF powder systems include HKUST-1 and UiO-66.

BASF's successful experience identifies the primary cost determinants of MOFs as: (1) the expense of the linker, (2) the spatiotemporal yield, (3) the work required for downstream processing, and (4) the solvent employed. Linkers are a commodity priced between less than 5 euros per kilogram and 100 euros per kilogram. The selected alternative will be dictated by the application and subsequent requirements for performance, cost, and pricing. The academic community has enhanced the process by increasing the concentration and reducing the reaction time, achieving a spatio-temporal yield exceeding 10 000 kg m<sup>-3</sup>, which is tenfold greater than the existing zeolite synthesis. The spatio-temporal yield is frequently diminished when downstream processes, including filtration, washing, drying, grinding, and molding, are

considered. BASF examined the production processes of several MOFs to ascertain the impact of each step on the quality of the final product. Continuous optimization has produced synthetic formulations that substitute organic solvents with water or altogether eliminate their necessity, thereby improving safety and further reducing costs.

Substantial advancements have been made in enhancing process efficiencies, lowering MOF production costs, and mitigating the dangers associated with large-scale manufacture. MOFs have exited the laboratory and are progressing towards commercial viability. BASF's experience indicates that the primary challenges lie in selecting appropriate MOFs for certain applications rather than scaling up the MOFs. Owing to the abundance of available MOFs and numerous theoretical MOF structures, computer-based simulations will become increasingly vital in the material selection process, facilitating a reduction in the development cycle and enhancing the likelihood of success.

**3.3.2 Repeated properties of MOFs to remove radioactive ions.** MOFs have become a prominent subject in wastewater treatment research because of their numerous active sites, high specific surface area, and versatile pore geometry. Unfortunately, MOFs and their composites/derivatives are typically provided in powder form, which may result in adverse disposal and recycling issues in industrial settings, potentially leading to powder contamination in certain instances.<sup>70</sup> The development of framework systems for reusable MOFs is crucial for enhancing the application of their properties. The recoverability of the MOF for various radioactive pollutants was examined, as shown in Fig. 6. Fig. 6 analyzes the frequency of radioactive element reuse with various eluents and the subsequent decrease in the adsorption rate after the specified number of cycles. The picture demonstrated that the eluents were

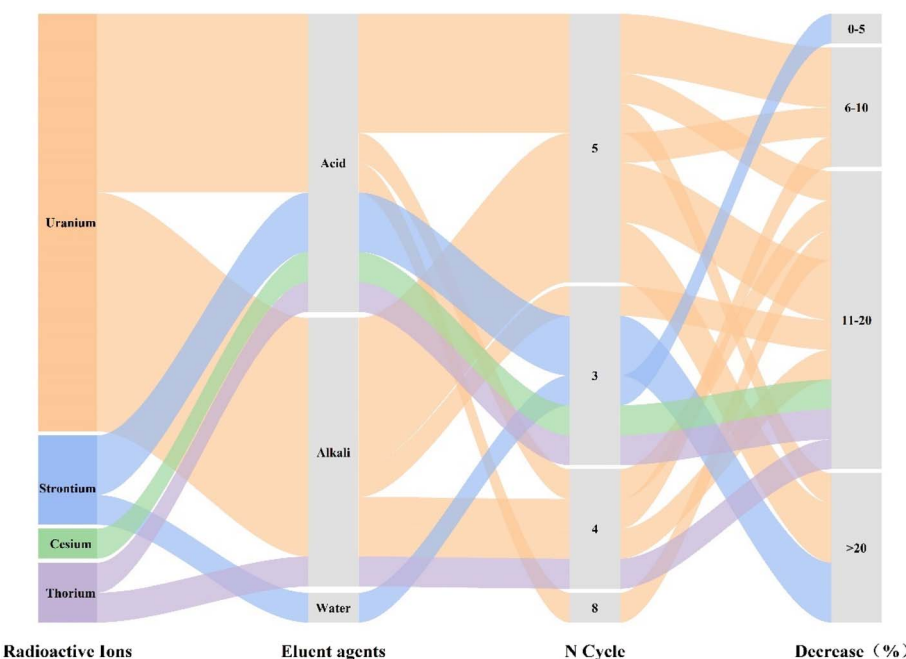


Fig. 6 Reusability of different radioactive elements.



categorized into three types: acids, bases, and water, suggesting that the adsorbent exhibited significant stability throughout the repeated adsorption and desorption cycles of radioactive elements with various desorbents. In the adsorption–elution cycles for radioactive pollutants, it is typical to attain over three cycles, with certain adsorbents capable of achieving eight cycles, while a negligible percentage can complete only two cycles. The considerable durability of the adsorbents was demonstrated by the observation that most adsorption rates diminished by less than 20 percent following the last elution cycle.

In solid–liquid separation, a preparation method that facilitates the recovery of MOF-based magnetic and device materials is crucial, alongside stability. The application of magnetic fields for the recovery of MOFs presents a promising solution to the current obstacles hindering their practical utilization.<sup>71</sup> Magnetic MOFs can be swiftly isolated and rapidly extracted using magnetic forces, eliminating the need for laborious filtration or centrifugation methods. Furthermore, these materials can be repurposed after washing, desorption, and regeneration, significantly reducing wastewater treatment costs. Co-MOFs impregnated with I<sub>2</sub> are subjected to multiple washes with ethanol to eliminate surplus I<sub>2</sub> from their surfaces, and the recovered material can be reused in the adsorption process for a minimum of five cycles.<sup>72</sup> Subsequently, the I<sub>2</sub> adsorption efficiency diminished somewhat, whereas no substantial reduction in the adsorption capacity was noted for Co-MOFs, even after five cycles. FCK(4)/ZIF-67(Co) showed the capability for reuse up to three times in the adsorption of Sr<sup>2+</sup> without substantial deactivation; however, the adsorbent exhibited considerable deactivation post-use relative to the original material.<sup>73</sup> Nevertheless, the majority of MOF-based compounds are intrinsically non-magnetic and require recombination with other magnetic adsorbents for reuse, which is aided by an external magnetic field. Compounds generated from MOFs with Fe<sup>3+</sup>, Co<sup>2+</sup>, and Ni<sup>2+</sup> frequently exhibit magnetic characteristics owing to the reduction of these magnetic ions to metallic states by hyperthermic carbothermal reduction in an inert environment or the creation of magnetic high-valent oxides in the presence of oxygen. The magnetic characteristics of MOF-based compounds are primarily obtained by the production of magnetic substances and pyrolysis of MOF precursors containing magnetic ions. Magnetic nanoparticles integrated with metal–organic frameworks (MOFs) show promise for pollutant sequestration. This study developed a magnetic metal–organic framework composite (Fe<sub>3</sub>O<sub>4</sub>@AMCA-MIL53 (Al)) for the extraction of Th(IV) and U(VI) metal ions from aqueous solutions.<sup>74</sup> The loading capabilities for UO<sub>2</sub><sup>2+</sup> and Th<sup>4+</sup> were quantified as 227.3 mg g<sup>-1</sup> and 285.7 mg g<sup>-1</sup>, respectively. The kinetic analysis revealed that the equilibrium time for each metal ion was 90 min. A range of thermodynamic properties was analyzed to determine the endothermic nature and spontaneity of the loading. The results demonstrate that Fe<sub>3</sub>O<sub>4</sub>@AMCA-MIL53 (Al) is an effective compound for the extraction of metal ions from water. Desorption with 0.01 M HCl efficiently recovered the deposited metal.

The utilization of magnetism for the recovery of MOFs, together with the amalgamation of MOFs and other polymeric substances into recyclable MOF devices featuring distinct macrostructures, effectively addresses the constraints associated with powdered MOFs in realistic purification applications. Devices with recyclable metal–organic frameworks (MOFs) typically include two-dimensional (2D) membrane composites and three-dimensional (3D) composites, such as beads, gels, sponges, and foams. A direct filtering technique was utilized to create a unique self-assembled membrane comprising MOF nanoribbons and GO.<sup>75</sup> The absorbing ability and effectiveness of the GO/Ni-MOF compound membrane for removing Sr<sup>2+</sup> from an aqueous environment are associated with the MOF concentration in the composite membrane. This study investigated the electrostatic interactions between Sr<sup>2+</sup> and oxygen-containing functional groups (O=C=O and C=O) in graphene oxide, physical adsorption *via* porous structures of MOF and GO/MOF interlaced channels, and the substitution of Ni<sup>2+</sup> inside MOF frameworks. The GO/Ni-MOF membrane exhibited a maximum adsorption performance of 72 mg g<sup>-1</sup> for Sr<sup>2+</sup> at pH 7. The GO/Ni-MOF composite membrane demonstrated high efficiency in Sr<sup>2+</sup> removal, cost-effectiveness, and simple synthesis, indicating substantial potential for use in radioactive contamination cleanup. Multifaceted MOF-on-MOF compounds, formed by the conjunction of various MOF units, exhibit greater complexity than single-component MOFs. These compounds display multiple attributes of a unique MOF structure, in addition to functions that a single-component MOF cannot provide.<sup>76</sup> A substance that absorbs water was synthesized using an epitaxial growth technique.<sup>77</sup> The findings demonstrated that the loading uptake of 2-MIL-101-on-NH<sub>2</sub>-UiO-66 for NH reached 80 mg g<sup>-1</sup>, with the adsorption rate increasing by 20–33%, and the adsorption capacity improving by 1.52–2.74 times. This adsorbent exceeds commercial silver-exchange zeolites and other MOF adsorbents in terms of its attributes. The remarkable adsorption capabilities of the adsorbent stem from its numerous adsorption sites and distinct pore architecture. The adsorbent exhibited thermal stability and could endure temperatures up to 360 °C. This investigation presents an extremely efficient compound for iodine removal and advances the understanding of unique MOF-on-MOF structures and their various uses.

**3.3.3 Biocompatibility of MOFs.** Fig. 7 illustrates that the choice of metal sources for MOFs utilized in addressing radioactive contaminants includes both heavy metal ions, such as Cr and Cd, and radioactive metal ions, such as Th<sup>4+</sup>. A key problem over the past decade has been the synthesis of MOFs that demonstrate exceptional stability, minimum adverse environmental impact, and outstanding performance. The minimal toxicity of both inorganic metals and organic ligands promotes the production of eco-friendly MOFs. High-valence metals such as Al<sup>3+</sup>, Zr<sup>4+</sup>, Fe<sup>3+</sup>, and Ti<sup>4+</sup> are abundant in nature and have stable compounds, rendering them non-toxic to humans. The incorporation of zirconium, a desirable metal in the formulation of MOFs owing to its superior non-toxicity, water stability, and cost-effective commercial accessibility, has attracted considerable attention.<sup>78</sup> The environmental impact of MOFs



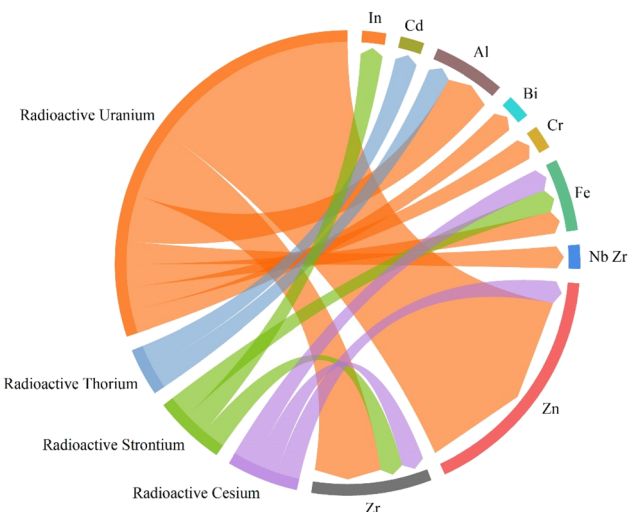


Fig. 7 Choice of metal sources for MOFs utilized in addressing radioactive contaminants.

can be significantly mitigated by employing biologically compatible organic linkers in their synthesis. Curcumin occurs naturally in the roots of turmeric, mustard, and curry, and in various other plants. It is a diaryl heptyl compound with free radical-scavenging and inhibitory characteristics.<sup>79</sup> High doses of curcumin (12 g day<sup>-1</sup>) are safe for human consumption.<sup>80</sup> The synthesized MOFs had a specific surface area of 3002 m<sup>2</sup> g<sup>-1</sup> and could withstand temperatures ranging from 350 to 450 °C. The yellow tint of the curcumin linker was observed in the MOFs. Nitrogen-containing functional group linkers are employed in the synthesis of MOFs with oxygen-containing functional group linkers, such as carboxylate or phenol. Amino acids, nucleotide bases, proteins, and peptides are examples of such molecules. Nitrogen-containing functional groups act as neutral double electron donors, offering an enhanced coordination environment for metal nodes without the charge-balancing constraints of conventional X-type ligands, such as carboxylates or alcohols. A recent study on the market analysis and economic synthesis of MOFs demonstrated the feasibility of large-scale production at a reduced cost.<sup>81</sup> The preparation of solvent-based MOFs poses risks to human health and may result in environmental problems. Conventional solvent-assisted MOF synthesis costs range from \$35 to \$71 per kilogram; however, solventless synthesis methods can be as economical as \$13 to \$36 per kilogram.<sup>82</sup> Considering all these factors, it is recommended that future metal-organic frameworks (MOFs) be synthesized by solvent-free and water-based methods, which will reduce manufacturing costs and mitigate toxicity.

Although the current methods for treating radioactive metal cations in nuclear wastewater have their own advantages, they all share significant limitations. The most prominent issues are the generation of secondary waste (such as sludge and waste resin), high operating costs, susceptibility of treatment efficiency to complex water quality, difficulties in scaling up, and challenges in long-term environmental risk management. To

address these problems, an innovative strategy has been proposed based on the fundamental characteristics of metal-organic frameworks (MOFs): using radioactive metal cations directly as the metal nodes of MOFs. In this process, these radioactive ions are no longer merely pollutants to be treated but instead serve as core raw materials, combining with organic ligands to form stable metal–oxygen clusters (M–O clusters), and through necessary structural modifications, ultimately constructing structurally stable MOF materials. This method of safely fixing radioactive metals and converting them into functional materials with potential applications represents an environmentally sustainable secondary utilization approach. Gao *et al.* synthesized semi-rigid monometallic catalysts utilizing Th-MOF-loaded  $\text{MCl}_2@\text{Th-BPYDC}$  ( $\text{M} = \text{Cu}, \text{Co}, \text{and Ni}$ ) through the post-metallization of bipyridyl Th-MOF (Th-BPYDC) crystals for acidic OER.<sup>83</sup> The Al/Th-MOF bimetallic organic framework removes fluorescent dye (FS) from the aqueous solution.<sup>84</sup> A Th-MOF-based artificial peroxidase was developed, which catalyzes the oxidation of 3,3,5,5-tetramethylbenzidine with hydrogen peroxide to generate a blue product. This is an exceptionally effective and sensitive colorimetric biosensor for detecting uric acid in biological materials.<sup>85</sup>

**3.3.4 Targeted adsorption ability of MOFs.** Overall, many of the materials demonstrated excellent interference resistance and target selectivity in the complex ionic environment of real water bodies. For example, in the screened reference, HNU-G6 maintained high removal rates at high salinity and high interference ions, which was attributed to the preferential selectivity of the amide moiety for U(vi). Even with a 100-fold increase in interfering ions, CAU-17 was able to remove 99.9% of uranium, which was attributed to the complexation of carboxylated oxygen atoms with uranium and charge modulation by bismuth. DUT-5-POR and DBT-DHTA-Cd showed good selectivity for uranium and thorium(iv), respectively, which was attributed to the phosphoramidic moiety, structural modification, and effect of the nanocavities containing hydroxyl and triazole nitrogen groups. DGIST-12 showed higher selectivity for divalent alkaline earth metal ions (*e.g.*, Sr<sup>2+</sup>), aided by its hydrophobic benzene portion, and MOF-303 proved to be suitable for the treatment of actual radioactive wastewater due to its excellent stability to  $\beta$ -irradiation. Materials such as ZIF-8/PAO, cCS/PVA/UiO-66-NH<sub>2</sub>, MILP-3, and ZIF-8/PEI effectively overcome the effect of interfering ions through specific functional groups (*e.g.*, amidoxime, amine, and unsaturated metal sites) or synergistic/improved strategies (*e.g.*, ZIF-8/PEI for anionic-cationic wastewater treatment), thus achieving efficient adsorption.

However, it must be pointed out that not all materials are completely immune to the influence of interfering ions. In some cases, such as UiO-66/AMP, the interfering ions can reduce the adsorption effect. Specifically, K<sup>+</sup> had a significant inhibitory effect on the adsorption of Cs(i) (whereas Na<sup>+</sup>, Mg<sup>2+</sup>, and Ca<sup>2+</sup> had little impact). When ZIF-8 immobilized on a loofah sponge was used to adsorb U(vi), although the overall efficiency remained above 87%, the influence of divalent Ca<sup>2+</sup> and Mg<sup>2+</sup> was greater than that of monovalent K<sup>+</sup> and Na<sup>+</sup>, possibly



because they are more likely to occupy active sites (although anions such as  $\text{Cl}^-$ ,  $\text{NO}_3^-$ , and  $\text{PO}_4^{3-}$  have little effect).  $\text{Nb}_3\text{C}_4@\text{UiO-66-NH}_2\text{-PA}$  showed selectivity for U(vi)/Eu(III) in wastewater, with a higher adsorption rate for U(vi), which is believed to be related to the difference in affinity caused by the higher valence state of uranium ions. Similarly, the maximum removal capacity of  $\text{Fe}_3\text{O}_4@\text{ZIF-8}$  for Eu(III) in seawater (high salinity and complex ions) was lower than that in other systems but still maintained a relatively high level.

In addition, some interesting phenomena were observed in this study. The adsorption capacity of  $\text{P-Al}_2\text{O}_3$  for U(vi) in synthetic groundwater was slightly higher than that in synthetic surface water, contrary to expectations, which is speculated to be related to the slight difference in the initial pH values. Notably, the adsorption effect of S-NZVI/UiO-66 in tap water and seawater was better than that in ultrapure water, indicating that the other ions present may promote the adsorption process, mainly through physical adsorption, electrostatic attraction, complexation, and reduction mechanisms.

## 4. Summary and prospects

In this study, a meta-analysis is performed to investigate the loading performance of MOFs in relation to radioactive elements, thereby providing a theoretical basis for evaluating the ecological and behavioral risks associated with the coexistence of these elements and MOFs. We systematically evaluated the influence of controlled variables (MOF properties and experimental conditions) on the loading of radioactive elements on MOFs, which significantly affects the capacity of adsorption, based on specific surface area, MOF stability, toxicity, and coexisting ions, while also considering the commercial value of the MOF. This is the most effective technique for integrating suitable functional groups onto MOFs and adjusting their pores to improve the metal ion selectivity and adsorption capacity. Notwithstanding significant advancements in radionuclide sequestration, MOFs continue to encounter hurdles and obstacles to practical implementation. Here are a few challenges.

(1) The impact of radiation on the stability of MOFs must be examined before their application in radioactive contexts. The efficacy of MOFs in aqueous solutions is often limited because they readily degrade under extreme alkaline and acidic conditions. The objective of this study was to create stable MOFs that are appropriate for a wide pH range, with special emphasis on their stability under aqueous and acidic/basic conditions. This is especially true if it is designed for nuclear waste management.

(2) Radionuclides manifest in various complex forms in the natural environment, including krypton (Kr), xenon (Xe), iodine vapor ( $\text{I}_2$ ), cations such as  $\text{Cs}^+$ ,  $\text{Sr}^{2+}$ , and  $\text{UO}_2^{2+}$ , and anions such as  $\text{TcO}_4^-$ . The adsorption process is linked to the adsorption efficiency of the MOFs. The structural designability of MOFs must be meticulously evaluated in the process of radionuclide removal, which is pertinent for the design of radioactive metal ion MOFs.

(3) The predominant method for preparing MOFs currently involves high-temperature and pressure conditions, which are time-consuming, complex, and constrained by significant

equipment limitations, rendering them unsuitable for large-scale commercial applications. Future studies should focus on the rapid synthesis of significant quantities of compounds at room temperature. The conversion of the metal salt and the type of solvent will not affect the synthesis of the target MOF, provided the metal center and the organic linker remain unchanged. This alleviates the time spent on laborious and intricate preliminary processes.

(4) Enhancing the reusability of MOFs is another method for decreasing their commercial cost. The greater the reuse of MOFs, the longer their lifespan and the lower the cost per utilization. A burgeoning body of research exists on this topic; however, few experiments have been adeptly designed to demonstrate repeatability, concentrating exclusively on the repetition rate per use while neglecting the critical desorption rate per use. The selection of an eluent is essential for the recycling of MOFs; the optimal eluent can effectively remove the adsorbed pollutants from the adsorbent while preserving its structural integrity, thereby facilitating the immediate reuse of MOFs.

(5) Radionuclides can serve as metal sources in MOF synthesis. By aligning with the HSAB theory based on the nuclide structure, it is possible to produce stable, non-water-soluble MOFs, thereby contributing to societal advancement and facilitating the conversion of waste into valuable resources.

(6) Metal-organic frameworks (MOFs) are not singular entities; their structural diversity and adaptability pose challenges for future advancements. A solitary MOF may be inadequate to meet the criteria for radioactive removal, while non-MOF alternatives may exhibit high selectivity for radionuclides, albeit with some shortcomings that must be addressed. Metal-organic frameworks (MOFs) can serve as carriers to combine with molecules such as crown ethers, facilitating the advantages of radionuclide capture.

(7) These studies have focused on the removal of single radioactive elements; however, in practical nuclear wastewater treatment, multiple radioactive elements often need to be treated simultaneously. Future studies should focus on the application of MOF materials in realistic aqueous environments.

The examination of adsorbents and technology for the uptake and extraction of radionuclides is essential for the progress of nuclear energy, significantly impacting human health and the global environment. To achieve this ideal objective, environmentalists, chemists, and materials scientists must interact effectively. Therefore, we support the thorough execution of policies and improved collaboration to reduce the hazards of Fanning radioactive contamination of marine ecosystems, the atmosphere, soil, and human health.

## Author contributions

Q.-L. Huang: investigation, writing – original draft, data curation, formal analysis, and visualization; X.-M. Chen: formal analysis and visualization. Q.-R. Zhang: editing, supervision, project administration, and conceptualization; J.-Y. Lim: data curation and conceptualization; S.-W. Zhao: data curation; H.-X.



Guan: visualization; S. Wang: resources and investigation; J.-Q. Liu: editing, supervision, conceptualization, and visualization.

## Conflicts of interest

The authors declare that they have no known competing financial interests or personal relationships.

## Data availability

The datasets utilized or examined in the present investigation can be obtained from the corresponding author upon reasonable inquiry.

Supplementary information is available. See DOI: <https://doi.org/10.1039/d5ta04304b>.

## Acknowledgements

This work was supported by the Jing-Jin-Ji Regional Integrated Environmental Improvement-National Science and Technology Major Project (2025ZD1205400 and 2025ZD1205401), the earmarked fund for the China Agriculture Research System (CARS-03) and the International Science & Technology Innovation Program of the Chinese Academy of Agricultural Sciences (CAAS-CFSGLCA-IEDA-202302 and CAAS-ZDRW202110). This work was funded by the Young Scientist Exchange Program between the People's Republic of China and the Republic of Korea. The authors acknowledge Hongzhiwei's assistance with technical communication and computer time support.

## References

- 1 T. Zhang, Q. Sun, W. Xiao, C. Luo and X. Liu, A Review on Emerging Mixed-Spectrum Nuclear Reactors for Safety and Sustainability of Nuclear Energy Systems, *Renew. Sustain. Energy Rev.*, 2024, **202**, 114666, DOI: [10.1016/j.rser.2024.114666](https://doi.org/10.1016/j.rser.2024.114666).
- 2 Y.-L. Liu, D. Li, P. Cao, X. Yin, Q. Zeng and H. Zhou, Advances in Mxene-Based Composite Materials for Efficient Removal of Radioactive Nuclides and Heavy Metal Ions, *Mater. Today Phys.*, 2024, **44**, 101444, DOI: [10.1016/j.mtphys.2024.101444](https://doi.org/10.1016/j.mtphys.2024.101444).
- 3 X. Liu, M. Xiao, Y. Li, Z. Chen, H. Yang and X. Wang, Advanced Porous Materials and Emerging Technologies for Radionuclides Removal from Fukushima Radioactive Water, *Eco-Environ. Health*, 2023, **2**(4), 252–256, DOI: [10.1016/j.eehl.2023.09.001](https://doi.org/10.1016/j.eehl.2023.09.001).
- 4 M. I. Ojovan, A. Pankov and W. E. Lee, The Ion Exchange Phase in Corrosion of Nuclear Waste Glasses, *J. Nucl. Mater.*, 2006, **358**(1), 57–68, DOI: [10.1016/j.jnucmat.2006.06.016](https://doi.org/10.1016/j.jnucmat.2006.06.016).
- 5 M. C. Duff, J. U. Coughlin and D. B. Hunter, Uranium Co-Precipitation with Iron Oxide Minerals, *Geochim. Cosmochim. Acta*, 2002, **66**(20), 3533–3547, DOI: [10.1016/S0016-7037\(02\)00953-5](https://doi.org/10.1016/S0016-7037(02)00953-5).
- 6 H. Ding, X. Zhang, H. Yang, Y. Zhang and X. Luo, Biosorption of U(Vi) by Active and Inactive *Aspergillus Niger*: Equilibrium, Kinetic, Thermodynamic and Mechanistic Analyses, *J. Radioanal. Nucl. Chem.*, 2019, **319**(3), 1261–1275, DOI: [10.1007/s10967-019-06420-0](https://doi.org/10.1007/s10967-019-06420-0).
- 7 K. Zhu, S. Lu, Y. Gao, R. Zhang, X. Tan and C. Chen, Fabrication of Hierarchical Core-Shell Polydopamine@MgAl-Ldhs Composites for the Efficient Enrichment of Radionuclides, *Appl. Surf. Sci.*, 2017, **396**, 1726–1735, DOI: [10.1016/j.apsusc.2016.11.230](https://doi.org/10.1016/j.apsusc.2016.11.230).
- 8 S. Tripatanasuwan, Z. Zhong and D. H. Reneker, Effect of Evaporation and Solidification of the Charged Jet in Electrospinning of Poly(Ethylene Oxide) Aqueous Solution, *Polymer*, 2007, **48**(19), 5742–5746, DOI: [10.1016/j.polymer.2007.07.045](https://doi.org/10.1016/j.polymer.2007.07.045).
- 9 C. Zhou, A. Ontiveros-Valencia, L. Cornette de Saint Cyr, A. S. Zevin, S. E. Carey, R. Krajmalnik-Brown and B. E. Rittmann, Uranium Removal and Microbial Community in a H<sub>2</sub>-Based Membrane Biofilm Reactor, *Water Res.*, 2014, **64**, 255–264, DOI: [10.1016/j.watres.2014.07.013](https://doi.org/10.1016/j.watres.2014.07.013).
- 10 Y. Mao, V. R. Ardham, L. Xu, P. Cui and D. Wu, Insight into Electrosorption Behavior of Monovalent Ions and Their Selectivity in Capacitive Deionization: An Atomic Level Study by Molecular Dynamics Simulation, *Chem. Eng. J.*, 2021, **415**, 128920, DOI: [10.1016/j.cej.2021.128920](https://doi.org/10.1016/j.cej.2021.128920).
- 11 S. D. Datar, S. Raheman, R. S. Mane, D. Chavda and N. Jha, Improved Electrosorption Performance Using Acid Treated Electrode Scaffold in Capacitive Deionization, *Mater. Chem. Phys.*, 2022, **281**, 125851, DOI: [10.1016/j.matchemphys.2022.125851](https://doi.org/10.1016/j.matchemphys.2022.125851).
- 12 M. Dai, L. Xia, S. Song, C. Peng, J. R. Rangel-Mendez and R. Cruz-Gaona, Electrosorption of as(iii) in Aqueous Solutions with Activated Carbon as the Electrode, *Appl. Surf. Sci.*, 2018, **434**, 816–821, DOI: [10.1016/j.apsusc.2017.10.238](https://doi.org/10.1016/j.apsusc.2017.10.238).
- 13 S. Huang and B. O. Oluyede, Exponentiated Kumaraswamy-Dagum Distribution with Applications to Income and Lifetime Data, *J. Stat. Distrib. Appl.*, 2014, **1**(1), 8, DOI: [10.1186/2195-5832-1-8](https://doi.org/10.1186/2195-5832-1-8).
- 14 K. Patra and A. Sengupta, Recent Advances in Functionalized Porous Adsorbents for Radioactive Waste Water Decontamination: Current Status, Research Gap and Future Outlook, *Mater. Today Sustain.*, 2024, **25**, 100703, DOI: [10.1016/j.mtsust.2024.100703](https://doi.org/10.1016/j.mtsust.2024.100703).
- 15 D. B. Tripathy, Recent Advances on 2d Metal Organic Framework (Mof) Membrane for Waste Water Treatment and Desalination, *Desalination*, 2024, **592**, 118183, DOI: [10.1016/j.desal.2024.118183](https://doi.org/10.1016/j.desal.2024.118183).
- 16 J. Zhang, D. Liu, X. Wang, Z. Zheng, J. Hu and Z. Chen, Efficient Uranium Removal from Radioactive Wastewater Using a Mof-Based Adsorbent Functionalized with Amidoxime, *J. Mol. Liq.*, 2025, **419**, 126759, DOI: [10.1016/j.molliq.2024.126759](https://doi.org/10.1016/j.molliq.2024.126759).
- 17 G. Wang, Q. Zhang, L. Qin, K. Tan, C. Li, L. Li, T. Yang and X. Liu, Construction of Mil-100(Fe)-Dma Material for Efficient Adsorption of Sr and Cs Ions from Radioactive Wastewater, *Sci. Total Environ.*, 2024, **954**, 176296, DOI: [10.1016/j.scitotenv.2024.176296](https://doi.org/10.1016/j.scitotenv.2024.176296).



18 H. Zhang, Y. Chi, J. Li, J. Peng, H. Song, C. Chen and X. Bai, Enhanced Adsorption of Radioactive Cesium from Nuclear Wastewater Using Zif-67 Laminated 2d Mxene Ti<sub>3</sub>c<sub>2</sub>, *Sep. Purif. Technol.*, 2025, 355, 129590, DOI: [10.1016/j.seppur.2024.129590](https://doi.org/10.1016/j.seppur.2024.129590).

19 M. Kaur, S. Kumar, M. Yusuf, J. Lee, A. K. Malik, Y. Ahmadi and K.-H. Kim, Schiff Base-Functionalized Metal-Organic Frameworks as an Efficient Adsorbent for the Decontamination of Heavy Metal Ions in Water, *Environ. Res.*, 2023, 236, 116811, DOI: [10.1016/j.envres.2023.116811](https://doi.org/10.1016/j.envres.2023.116811).

20 I. Ahmed, M. M. H. Mondol, H. J. Lee and S. H. Jhung, Application of Metal-Organic Frameworks in Adsorptive Removal of Organic Contaminants from Water, Fuel and Air, *Chem.-Asian J.*, 2021, 16(3), 185–196, DOI: [10.1002/asia.202001365](https://doi.org/10.1002/asia.202001365).

21 E. Barea, C. Montoro and J. A. R. Navarro, Toxic Gas Removal – Metal-Organic Frameworks for the Capture and Degradation of Toxic Gases and Vapours, *Chem. Soc. Rev.*, 2014, 43(16), 5419–5430, DOI: [10.1039/C3CS60475F](https://doi.org/10.1039/C3CS60475F).

22 N. A. Khan, Z. Hasan and S. H. Jhung, Adsorptive Removal of Hazardous Materials Using Metal-Organic Frameworks (Mofs): A Review, *J. Hazard Mater.*, 2013, 244–245, 444–456, DOI: [10.1016/j.jhazmat.2012.11.011](https://doi.org/10.1016/j.jhazmat.2012.11.011).

23 Y. Zhang, M. Ren, Y. Tang, X. Cui, J. Cui, C. Xu, H. Qie, X. Tan, D. Liu, J. Zhao, S. Wang and A. Lin, Immobilization on Anionic Metal(Loid)S in Soil by Biochar: A Meta-Analysis Assisted by Machine Learning, *J. Hazard Mater.*, 2022, 438, 129442, DOI: [10.1016/j.jhazmat.2022.129442](https://doi.org/10.1016/j.jhazmat.2022.129442).

24 S. Bi, S. Liu, E. Liu, J. Xiong, Y. Xu, R. Wu, X. Liu and J. Xu, Adsorption Behavior and Mechanism of Heavy Metals onto Microplastics: A Meta-Analysis Assisted by Machine Learning, *Environ. Pollut.*, 2024, 360, 124634, DOI: [10.1016/j.envpol.2024.124634](https://doi.org/10.1016/j.envpol.2024.124634).

25 L. V. Hedges, J. Gurevitch and P. S. Curtis, The Meta-Analysis of Response Ratios in Experimental Ecology, *Ecology*, 1999, 80(4), 1150–1156, DOI: [10.1890/0012-9658\(1999\)080\[1150:TMAORR\]2.0.CO;2](https://doi.org/10.1890/0012-9658(1999)080[1150:TMAORR]2.0.CO;2).

26 W. Van Den Noortgate and P. Onghena, Parametric and Nonparametric Bootstrap Methods for Meta-Analysis, *Behav. Res. Methods*, 2005, 37(1), 11–22, DOI: [10.3758/BF03206394](https://doi.org/10.3758/BF03206394).

27 E. A. Ainsworth, Rice Production in a Changing Climate: A Meta-Analysis of Responses to Elevated Carbon Dioxide and Elevated Ozone Concentration, *Glob. Change Biol.*, 2008, 14(7), 1642–1650, DOI: [10.1111/j.1365-2486.2008.01594.x](https://doi.org/10.1111/j.1365-2486.2008.01594.x).

28 P. B. Morgan, E. A. Ainsworth and S. P. Long, How Does Elevated Ozone Impact Soybean? A Meta-Analysis of Photosynthesis, Growth and Yield, *Plant, Cell Environ.*, 2003, 26(8), 1317–1328, DOI: [10.1046/j.0016-8025.2003.01056.x](https://doi.org/10.1046/j.0016-8025.2003.01056.x).

29 W. J. Liu, G. Y. Hong, D. D. Dai, L. M. Li and M. Dolg, The Beijing Four-Component Density Functional Program Package (Bdf) and Its Application to Eu<sub>0</sub>, Eu<sub>5</sub>, Yb<sub>0</sub> and Yb<sub>5</sub>, *Theor. Chem. Acc.*, 1997, 96(2), 75–83, DOI: [10.1007/s002140050207](https://doi.org/10.1007/s002140050207).

30 Y. Zhang, B. Suo, Z. Wang, N. Zhang, Z. Li, Y. Lei, W. Zou, J. Gao, D. Peng, Z. Pu, Y. Xiao, Q. Sun, F. Wang, Y. Ma, X. Wang, Y. Guo and W. Liu, Bdf: A Relativistic Electronic Structure Program Package, *J. Chem. Phys.*, 2020, 152(6), 064113, DOI: [10.1063/1.5143173](https://doi.org/10.1063/1.5143173).

31 W. J. Liu, F. Wang and L. M. Li, The Beijing Density Functional (Bdf) Program Package: Methodologies and Applications, *J. Theor. Comput. Chem.*, 2003, 2(2), 257–272, DOI: [10.1142/s0219633603000471](https://doi.org/10.1142/s0219633603000471).

32 T. Lu, A Comprehensive Electron Wavefunction Analysis Toolbox for Chemists, Multiwfn, *J. Chem. Phys.*, 2024, 161(8), 082503, DOI: [10.1063/5.0216272](https://doi.org/10.1063/5.0216272).

33 T. Lu and F. Chen, Multiwfn: A Multifunctional Wavefunction Analyzer, *J. Comput. Chem.*, 2012, 33(5), 580–592, DOI: [10.1002/jcc.22885](https://doi.org/10.1002/jcc.22885).

34 W. Humphrey, A. Dalke and K. Schulten, Vmd: Visual Molecular Dynamics, *J. Mol. Graphics Modell.*, 1996, 14(1), 33–38, DOI: [10.1016/0263-7855\(96\)00018-5](https://doi.org/10.1016/0263-7855(96)00018-5).

35 <https://www.ks.uiuc.edu/Research/vmd/>.

36 C. E. Wilmer, M. Leaf, C. Y. Lee, O. K. Farha, B. G. Hauser, J. T. Hupp and R. Q. Snurr, Large-Scale Screening of Hypothetical Metal-Organic Frameworks, *Nat. Chem.*, 2012, 4(2), 83–89, DOI: [10.1038/nchem.1192](https://doi.org/10.1038/nchem.1192).

37 T. He, X.-J. Kong and J.-R. Li, Chemically Stable Metal-Organic Frameworks: Rational Construction and Application Expansion, *Acc. Chem. Res.*, 2021, 54(15), 3083–3094, DOI: [10.1021/acs.accounts.1c00280](https://doi.org/10.1021/acs.accounts.1c00280).

38 X. Zhang, B. Wang, A. Alsalme, S. Xiang, Z. Zhang and B. Chen, Design and Applications of Water-Stable Metal-Organic Frameworks: Status and Challenges, *Coord. Chem. Rev.*, 2020, 423, 213507, DOI: [10.1016/j.ccr.2020.213507](https://doi.org/10.1016/j.ccr.2020.213507).

39 L. Wang, X. Li, B. Yang, K. Xiao, H. Duan and H. Zhao, The Chemical Stability of Metal-Organic Frameworks in Water Treatments: Fundamentals, Effect of Water Matrix and Judging Methods, *Chem. Eng. J.*, 2022, 450, 138215, DOI: [10.1016/j.cej.2022.138215](https://doi.org/10.1016/j.cej.2022.138215).

40 S. Yuan, L. Feng, K. Wang, J. Pang, M. Bosch, C. Lollar, Y. Sun, J. Qin, X. Yang, P. Zhang, Q. Wang, L. Zou, Y. Zhang, L. Zhang, Y. Fang, J. Li and H.-C. Zhou, Stable Metal-Organic Frameworks: Design, Synthesis, and Applications, *Adv. Mater.*, 2018, 30(37), 1704303, DOI: [10.1002/adma.201704303](https://doi.org/10.1002/adma.201704303).

41 M. Du, G. Xu, J. Zhang, Y. Guan, C. Guo and Y. Chen, Hierarchically Porous Mil-100(Fe) with Large Mesopores for Cationic Dye Adsorption, *J. Solid State Chem.*, 2023, 322, 123950, DOI: [10.1016/j.jssc.2023.123950](https://doi.org/10.1016/j.jssc.2023.123950).

42 N. H. M. H. Tehrani, M. S. Alivand, A. Kamali, M. D. Esrafil, M. Shafiei-Alavijeh, R. Ahmadi, M. Samipoorgiri, O. Tavakoli and A. Rashidi, Seed-Mediated Synthesis of a Modified Micro-Mesoporous Mil-101(Cr) for Improved Benzene and Toluene Adsorption at Room Conditions, *J. Environ. Chem. Eng.*, 2023, 11(3), 109558, DOI: [10.1016/j.jece.2023.109558](https://doi.org/10.1016/j.jece.2023.109558).

43 L. Ding, M. Xiong, X. Yin, L. Fang, L. Liu, W. Ren, F. Deng and X. Luo, Post-Modified Ligand Exchange of Uio-66 with High-Exposure Rhodanine Sites for Enhancing the Rapid and Selective Capture of Ag(I) from Wastewater, *Sep. Purif.*



Technol., 2023, **314**, 123541, DOI: [10.1016/j.seppur.2023.123541](https://doi.org/10.1016/j.seppur.2023.123541).

44 D. Yang and B. C. Gates, Analyzing Stabilities of Metal-Organic Frameworks: Correlation of Stability with Node Coordination to Linkers and Degree of Node Metal Hydrolysis, *J. Phys. Chem. C*, 2024, **128**(21), 8551–8559, DOI: [10.1021/acs.jpcc.4c02105](https://doi.org/10.1021/acs.jpcc.4c02105).

45 M. Wang, Y. Sun, C. Huang, P. Wang, H. Cheng, C. Sun, D. Jiang, D. Ling, K. Ouyang and C. Feng, Nanoporous Anodic Aluminum Oxide-Confined Zif-67 for Efficiently Activating Peroxymonosulfate to Degrade Organic Pollutants, *Sep. Purif. Technol.*, 2023, **318**, 123946, DOI: [10.1016/j.seppur.2023.123946](https://doi.org/10.1016/j.seppur.2023.123946).

46 C. Guo, M. Yuan, L. He, L. Cheng, X. Wang, N. Shen, F. Ma, G. Huang and S. Wang, Efficient capture of  $\text{Sr}^{2+}$  from acidic aqueous solution by an 18-crown-6-ether-based metal organic framework, *CrystEngComm*, 2021, **23**(18), 3349–3355, DOI: [10.1039/d1ce00229e](https://doi.org/10.1039/d1ce00229e).

47 D. Song, J. Bae, H. Ji, M.-B. Kim, Y.-S. Bae, K. S. Park, D. Moon and N. C. Jeong, Coordinative Reduction of Metal Nodes Enhances the Hydrolytic Stability of a Paddlewheel Metal-Organic Framework, *J. Am. Chem. Soc.*, 2019, **141**(19), 7853–7864, DOI: [10.1021/jacs.9b02114](https://doi.org/10.1021/jacs.9b02114).

48 J. M. Taylor, R. Vaidhyanathan, S. S. Iremonger and G. K. H. Shimizu, Enhancing Water Stability of Metal-Organic Frameworks Via Phosphonate Monoester Linkers, *J. Am. Chem. Soc.*, 2012, **134**(35), 14338–14340, DOI: [10.1021/ja306812r](https://doi.org/10.1021/ja306812r).

49 Z. He, H. Wu, Z. Shi, X. Duan, S. Ma, J. Chen, Z. Kong, A. Chen, Y. Sun and X. Liu, Mussel-Inspired Durable Superhydrophobic/Superoleophilic Mof-Pu Sponge with High Chemical Stability, Efficient Oil/Water Separation and Excellent Anti-Icing Properties, *Colloids Surf. A*, 2022, **648**, 129142, DOI: [10.1016/j.colsurfa.2022.129142](https://doi.org/10.1016/j.colsurfa.2022.129142).

50 S. Liu, P. Li, Y. Zhang, X. Gao, G. Wang, S. Song and X. Zhao, Hydrophobic Mof-808 Particles Encapsulated Melamine Sponge for Efficient Oil-Water Separation, *Environ. Funct. Mater.*, 2024, **3**(1), 25–33, DOI: [10.1016/j.efmat.2024.07.004](https://doi.org/10.1016/j.efmat.2024.07.004).

51 S. Bureekaew and R. Schmid, Hypothetical 3d-Periodic Covalent Organic Frameworks: Exploring the Possibilities by a First Principles Derived Force Field, *CrystEngComm*, 2013, **15**(8), 1551–1562, DOI: [10.1039/c2ce26473k](https://doi.org/10.1039/c2ce26473k).

52 Y. G. Chung, J. Camp, M. Haranczyk, B. J. Sikora, W. Bury, V. Krungleviciute, T. Yildirim, O. K. Farha, D. S. Sholl and R. Q. Snurr, Computation-Ready, Experimental Metal-Organic Frameworks: A Tool to Enable High-Throughput Screening of Nanoporous Crystals, *Chem. Mater.*, 2014, **26**(21), 6185–6192, DOI: [10.1021/cm502594j](https://doi.org/10.1021/cm502594j).

53 G. Maurin, Role of Molecular Simulations in the Structure Exploration of Metal-Organic Frameworks: Illustrations through Recent Advances in the Field, *C. R. Chim.*, 2016, **19**(1–2), 207–215, DOI: [10.1016/j.cre.2015.07.013](https://doi.org/10.1016/j.cre.2015.07.013).

54 J. S. Murray, F. Abu-Awwad and P. Politzer, Prediction of Aqueous Solvation Free Energies from Properties of Solute Molecular Surface Electrostatic Potentials, *J. Phys. Chem. A*, 1999, **103**(12), 1853–1856, DOI: [10.1021/jp984271w](https://doi.org/10.1021/jp984271w).

55 X. Chen, X. Liu, S. Xiao, W. Xue, X. Zhao and Q. Yang, A B-Ray Irradiation Resistant Mof-Based Trap for Efficient Capture of Th(IV) Ion, *Sep. Purif. Technol.*, 2022, **297**, 121517, DOI: [10.1016/j.seppur.2022.121517](https://doi.org/10.1016/j.seppur.2022.121517).

56 C. Ma, H. Liu, H. T. Wolterbeek, A. G. Denkova and P. Serra Crespo, Effects of High Gamma Doses on the Structural Stability of Metal-Organic Frameworks, *Langmuir*, 2022, **38**(29), 8928–8933, DOI: [10.1021/acs.langmuir.2c01074](https://doi.org/10.1021/acs.langmuir.2c01074).

57 S. Ma, Z. Zhou, Y. Zhang, R. Rao, H. Han, J. Liang, Z. Zhao, F. Bi, N. Liu and X. Zhang, Review of Irradiation Treatments on Mofs and Cofs: Synthesis, Modification, and Application, *Sep. Purif. Technol.*, 2024, **339**, 126636, DOI: [10.1016/j.seppur.2024.126636](https://doi.org/10.1016/j.seppur.2024.126636).

58 F. Marinkovic, B. Skipina, D. Vukovic, E. H. G. Langner, A. S. Luyt and D. Dudic, Ac Conductivity of Gamma Irradiated Ldpe/Zif-8 Composite, *J. Macromol. Sci., Part B: Phys.*, 2022, **61**(10–11), 1261–1269, DOI: [10.1080/00222348.2022.2159697](https://doi.org/10.1080/00222348.2022.2159697).

59 A. G. Al Lafi, B. Assfour and T. Assaad, Spectroscopic Investigations of Gamma-Ray Irradiation Effects on Metal Organic Framework, *J. Mater. Sci.*, 2021, **56**(21), 12154–12170, DOI: [10.1007/s10853-021-06051-5](https://doi.org/10.1007/s10853-021-06051-5).

60 P. Markopoulou and R. S. Forgan, Postsynthetic Modification of Mofs for Biomedical Applications, *Met.-Org. Frameworks Biomed. Appl.*, 2020, 245–276, DOI: [10.1016/b978-0-12-816984-1.00014-7](https://doi.org/10.1016/b978-0-12-816984-1.00014-7).

61 S. Liu, J. Zu, G. Han, X. Pan, Y. Xue, J. Diao, Q. Tang and M. Jin, Ammonium Phosphomolybdate-Modified Uio-66 as an Efficient Adsorbent for the Selective Removal of  $^{137}\text{Cs}$  from Radioactive Wastewater, *Sep. Purif. Technol.*, 2024, **329**, 125073, DOI: [10.1016/j.seppur.2023.125073](https://doi.org/10.1016/j.seppur.2023.125073).

62 K. Sang, D. Mei, Y. Wang, L. Liu, H. Li, G. Yang, F. Ma, C. Zhang and H. Dong, Amidoxime-Functionalized Zeolitic Imidazolate Frameworks with Antimicrobial Property for the Removal of U (VI) from Wastewater, *J. Environ. Chem. Eng.*, 2022, **10**(5), 108344, DOI: [10.1016/j.jece.2022.108344](https://doi.org/10.1016/j.jece.2022.108344).

63 L. Ren, X. Zhao, B. Liu and H. Huang, Synergistic Effect of Carboxyl and Sulfate Groups for Effective Removal of Radioactive Strontium Ion in a Zr-Metal-Organic Framework, *Water Sci. Technol.*, 2021, **83**(8), 2001–2011, DOI: [10.2166/wst.2021.103](https://doi.org/10.2166/wst.2021.103).

64 L. Quynh Thi Ngoc and K. Cho, Caesium Adsorption on a Zeolitic Imidazolate Framework (Zif-8) Functionalized by Ferrocyanide, *J. Colloid Interface Sci.*, 2021, **581**, 741–750, DOI: [10.1016/j.jcis.2020.08.017](https://doi.org/10.1016/j.jcis.2020.08.017).

65 Q. T. N. Le and K. Cho, Caesium Adsorption on a Zeolitic Imidazolate Framework (Zif-8) Functionalized by Ferrocyanide, *J. Colloid Interface Sci.*, 2021, **581**, 741–750, DOI: [10.1016/j.jcis.2020.08.017](https://doi.org/10.1016/j.jcis.2020.08.017).

66 S. Diao, M. Li, X. Liu, Y. Liu, Q. Shang and Y. Xu, Ca/Mg Bimetallic Mofs Modified with Amidoximerized Polyacrylonitrile and High Efficiency Uranium(VI) Extraction from Solution, *J. Solid State Chem.*, 2024, **338**, 124894, DOI: [10.1016/j.jssc.2024.124894](https://doi.org/10.1016/j.jssc.2024.124894).

67 Z. Li, M. Zhou, S. Wang and B. Hu, Fabrication of Amino-Functionalized Ce/Mn Bimetallic Organic Framework and Its Efficient Performance on Uranium(VI) Extraction in



Aqueous Solutions, *Sep. Purif. Technol.*, 2024, **345**, 127217, DOI: [10.1016/j.seppur.2024.127217](https://doi.org/10.1016/j.seppur.2024.127217).

68 Y. Zhang, H. Liu, F. Gao, X. Tan, Y. Cai, B. Hu, Q. Huang, M. Fang and X. Wang, Application of Mofs and Cofs for Photocatalysis in Co<sub>2</sub> Reduction, H<sub>2</sub> Generation, and Environmental Treatment, *EnergyChem*, 2022, **4**(4), 100078, DOI: [10.1016/j.enchem.2022.100078](https://doi.org/10.1016/j.enchem.2022.100078).

69 L. Chen, P. Xue, Q. Liang, X. Liu, J. Tang, J. Li, J. Liu, M. Tang and Z. Wang, A Single-Ion Polymer Composite Electrolyte Via in Situ Polymerization of Electrolyte Monomers into a Porous Mof-Based Fibrous Membrane for Lithium Metal Batteries, *ACS Appl. Energy Mater.*, 2022, **5**(3), 3800–3809, DOI: [10.1021/acsae.2c00282](https://doi.org/10.1021/acsae.2c00282).

70 N. Hammi, S. Chen, A. Primo, S. Royer, H. Garcia and A. El Kadib, Shaping Mof Oxime Oxidation Catalysts as Three-Dimensional Porous Aerogels through Structure-Directing Growth inside Chitosan Microspheres, *Green Chem.*, 2022, **24**(11), 4533–4543, DOI: [10.1039/d2gc00097k](https://doi.org/10.1039/d2gc00097k).

71 K. Wang, S. Zhang, R. Wang, Z. He, H. Chen and S.-H. Ho, Rational Design of Recyclable Metal-Organic Frameworks-Based Materials for Water Purification: An Opportunity for Practical Application, *Sci. Total Environ.*, 2023, **892**, 164345, DOI: [10.1016/j.scitotenv.2023.164345](https://doi.org/10.1016/j.scitotenv.2023.164345).

72 K. M. A. Qasem, S. Khan, M. N. Ahamad, H. A. M. Saleh, M. Ahmad and M. Shahid, Radioactive Iodine Capture by Metal Organic Frameworks in Liquid and Vapour Phases: An Experimental, Kinetic and Mechanistic Study, *J. Environ. Chem. Eng.*, 2021, **9**(6), 106720, DOI: [10.1016/j.jece.2021.106720](https://doi.org/10.1016/j.jece.2021.106720).

73 Z. W. Wang, H. Zhang, H. Y. Song and X. F. Bai, Ultra-Fine Potassium Hexacyanoferrate(II) Nanoparticles Modified Zif-67 for Adsorptive Removal of Radioactive Strontium from Nuclear Wastewater, *Sep. Purif. Technol.*, 2024, **331**, 125587, DOI: [10.1016/j.seppur.2023.125587](https://doi.org/10.1016/j.seppur.2023.125587).

74 A. A. Alqadami, M. Naushad, Z. A. Alothman and A. A. Ghfar, Novel Metal-Organic Framework (Mof) Based Composite Material for the Sequestration of U(Vi) and Th(IV) Metal Ions from Aqueous Environment, *ACS Appl. Mater. Interfaces*, 2017, **9**(41), 36026–36037, DOI: [10.1021/acsami.7b10768](https://doi.org/10.1021/acsami.7b10768).

75 J. Y. Cheng, K. L. Liu, X. Li, L. Huang, J. Liang, G. P. Zheng and G. C. Shan, Nickel-Metal-Organic Framework Nanobelt Based Composite Membranes for Efficient Sr<sup>2+</sup> Removal from Aqueous Solution, *Environ. Sci. Ecotechnology*, 2020, **3**, 100035, DOI: [10.1016/j.esce.2020.100035](https://doi.org/10.1016/j.esce.2020.100035).

76 M. S. Yao, J. W. Xiu, Q. Q. Huang, W. H. Li, W. W. Wu, A. Q. Wu, L. A. Cao, W. H. Deng, G. E. Wang and G. Xu, Van Der Waals Heterostructured Mof-on-Mof Thin Films: Cascading Functionality to Realize Advanced Chemiresistive Sensing, *Angew. Chem., Int. Ed.*, 2019, **58**(42), 14915–14919, DOI: [10.1002/anie.201907772](https://doi.org/10.1002/anie.201907772).

77 L. S. Liu, L. F. Chen, K. Thummavichai, Z. X. Ye, Y. B. Wang, T. Fujita and X. P. Wang, Amino-Functionalized Mof-on-Mof Architectural Nanocomplexes Composed for Radioactive-Iodine Efficient Adsorption, *Chem. Eng. J.*, 2023, **474**, 145858, DOI: [10.1016/j.cej.2023.145858](https://doi.org/10.1016/j.cej.2023.145858).

78 Y. Bai, Y. Dou, L.-H. Xie, W. Rutledge, J.-R. Li and H.-C. Zhou, Zr-Based Metal-Organic Frameworks: Design, Synthesis, Structure, and Applications, *Chem. Soc. Rev.*, 2016, **45**(8), 2327–2367, DOI: [10.1039/c5cs00837a](https://doi.org/10.1039/c5cs00837a).

79 H. Su, F. Sun, J. Jia, H. He, A. Wang and G. Zhu, A Highly Porous Medical Metal-Organic Framework Constructed from Bioactive Curcumin, *Chem. Commun.*, 2015, **51**(26), 5774–5777, DOI: [10.1039/c4cc10159f](https://doi.org/10.1039/c4cc10159f).

80 S. Sengupta, M. Sahoo, V. V. Sravani, B. Sreenivasulu, C. Rao and A. Suresh, Highly Efficient Post-Synthetically Modified Uio-66 Mof for the Extraction of Pd(II) from Aqueous Solutions: Experimental and Theoretical Studies, *New J. Chem.*, 2023, **47**(31), 14921–14932, DOI: [10.1039/d3nj02770h](https://doi.org/10.1039/d3nj02770h).

81 P. Kumar, A. Deep and K.-H. Kim, Metal Organic Frameworks for Sensing Applications, *TrAC, Trends Anal. Chem.*, 2015, **73**, 39–53, DOI: [10.1016/j.trac.2015.04.009](https://doi.org/10.1016/j.trac.2015.04.009).

82 D. DeSantis, J. A. Mason, B. D. James, C. Houchins, J. R. Long and M. Veenstra, Techno-Economic Analysis of Metal-Organic Frameworks for Hydrogen and Natural Gas Storage, *Energy Fuels*, 2017, **31**(2), 2024–2032, DOI: [10.1021/acs.energyfuels.6b02510](https://doi.org/10.1021/acs.energyfuels.6b02510).

83 Z. Gao, Y. L. Lai, L. L. Gong, L. P. Zhang, S. B. Xi, J. Sun, L. J. Zhang and F. Luo, Robust Th-Mof-Supported Semirigid Single-Metal-Site Catalyst for an Efficient Acidic Oxygen Evolution Reaction, *ACS Catal.*, 2022, **12**(15), 9101–9113, DOI: [10.1021/acscatal.2c02181](https://doi.org/10.1021/acscatal.2c02181).

84 N. A. H. Alshammari, J. S. Alnawmasi, A. M. Alotaibi, O. A. O. Alshammari, M. A. Abomuti, N. H. Elsayed and A. A. El-Binary, Efficient Adsorption of Fluorescein Dye from Aqueous Solutions by Al/Th-Mof Bimetal-Organic Frameworks: Adsorption Isotherm, Kinetics, Dft Computation, and Optimization Via Box-Behnken Design, *Process Saf. Environ. Prot.*, 2024, **190**, 1–19, DOI: [10.1016/j.psep.2024.08.037](https://doi.org/10.1016/j.psep.2024.08.037).

85 A. Badoei-dalfard, N. Sohrabi, Z. Karami and G. Sargazi, Fabrication of an Efficient and Sensitive Colorimetric Biosensor Based on Uricase/Th-Mof for Uric Acid Sensing in Biological Samples, *Biosens. Bioelectron.*, 2019, **141**, 111420, DOI: [10.1016/j.bios.2019.111420](https://doi.org/10.1016/j.bios.2019.111420).

